Noname manuscript No.
(will be inserted by the editor)

Extended Gauss-Newton and Gauss-Newton-ADMM Algorithms for Low-Rank Matrix Optimization

Quoc Tran-Dinh* · **Zheqi Zhang**

arXiv:1606.03358v2 [math.OC] 23 Aug 2016

Received: date / Accepted: date

Abstract We develop a generic Gauss-Newton (GN) framework for solving a class of nonconvex optimization problems involving low-rank matrix variables. As opposed to standard Gauss-Newton method, our framework allows one to handle general smooth convex cost function via its surrogate. The main complexity-per-iteration consists of the inverse of two rank-size matrices and at most six small matrix multiplications to compute a closed form Gauss-Newton direction, and a backtracking linesearch. We show, under mild conditions, that the proposed algorithm globally and locally converges to a stationary point of the original nonconvex problem. We also show empirically that the Gauss-Newton algorithm achieves much higher accurate solutions compared to the well studied alternating direction method (ADM). Then, we specify our Gauss-Newton framework to handle the symmetric case and prove its convergence, where ADM is not applicable without lifting variables.

Next, we incorporate our Gauss-Newton scheme into the alternating direction method of multipliers (ADMM) to design a GN-ADMM algorithm for solving the low-rank optimization problem. We prove that, under mild conditions and a proper choice of the penalty parameter, our GN-ADMM globally converges to a stationary point of the original problem. Finally, we apply our algorithms to solve several problems in practice such as low-rank approximation, matrix completion, robust low-rank matrix recovery, and matrix recovery in quantum tomography. The numerical experiments provide encouraging results to motivate the use of nonconvex optimization.

Keywords Low-rank approximation · Gauss-Newton method · Nonconvex alternating direction method of multipliers · quadratic and linear convergence · global convergence.

Mathematics Subject Classification (2000) 90C26 · 90-08

1 Introduction

Various practical models in low-rank embedded problems, function learning, matrix completion in recommender systems, inpainting and compression in image processing, robust principle component analysis in statistics, and semidefinite programming relaxations in combinatorial optimization often require to recover a low-rank matrix from

Q. Tran-Dinh · Z. Zhang
Department of Statistics and Operations Research, University of North Carolina at Chapel Hill, 333 Hanes Hall, UNC-Chapel Hill, NC-27599, USA. E-mail: quoctd@email.unc.edu

either given high-rank datasets or observations corrupted by noise. Such practical models can be formulated into low-rank matrix optimization problems, see, e.g., [10, 12, 14, 16, 27, 30, 40].

1.1 Problem statement

In this paper, we consider the following class of low-rank matrix optimization problems:

$$\Phi^\star := \min_{U,V} \left\{ \Phi(U,V) := \phi\left(\mathcal{A}(UV^T) - B\right) : U \in \mathbb{R}^{m\times r},\ V \in \mathbb{R}^{n\times r} \right\}, \tag{1}$$

where $\phi : \mathbb{R}^l \to \mathbb{R}\cup\{+\infty\}$ is a proper, closed and convex function; $\mathcal{A} : \mathbb{R}^{m\times n} \to \mathbb{R}^l$ is a linear operator, defined as $\mathcal{A}(Z) := [\mathrm{trace}\left(A_1^T Z\right), \mathrm{trace}\left(A_2^T Z\right), \cdots, \mathrm{trace}\left(A_l^T Z\right)]$ for l matrices $A_1, \cdots, A_l$ in $\mathbb{R}^{m\times n}$; and $B \in \mathbb{R}^l$ is an observed vector. We are interested in the low-rank case, where $r \ll \min\{m, n\}$.

Clearly, (1) is nonconvex due to the bilinear term UV^T. Hence, it is NP-hard [31], and numerical methods for solving (1) aim at obtaining a local optimum or a stationary point. While (1) covers a wide range of applications, we briefly recall some emerging problems which have been recently attracted a great attention. The most common case is when $\phi(\cdot) := (1/2)\|\cdot\|_2^2$, where (1) becomes a least-squares low-rank matrix approximation problem using in compressive sensing (see, e.g., [27]):

$$\min_{U,V} \left\{ (1/2)\|\mathcal{A}(UV^T) - B\|_2^2 : U \in \mathbb{R}^{m\times r}, V \in \mathbb{R}^{n\times r} \right\}. \tag{2}$$

Here, the linear operator $\mathcal{A}$ is often assumed to satisfy a restricted isometric property (RIP) [11] that allows us to recover an exact solution from a few number of observations in B. In particular, if $\mathcal{A} = \mathcal{P}_\Omega$, the projection on a given index subset Ω, then (2) covers the matrix completion model as a special case:

$$\min_{U,V} \left\{ (1/2)\|\mathcal{P}_\Omega(UV^T) - B_\Omega\|_F^2 : U \in \mathbb{R}^{m\times r}, V \in \mathbb{R}^{n\times r} \right\}, \tag{3}$$

where B_Ω is the observed entries in Ω. If $\mathcal{A}$ is an identity operator and $B \in \mathbb{R}^{m\times n}$ is a given low-rank matrix, then (2) becomes a low-rank matrix factorization problem

$$\Phi^\star := \min_{U,V} \left\{ \Phi(U,V) = (1/2)\|UV^T - B\|_F^2 \ :\ U \in \mathbb{R}^{m\times r},\ V \in \mathbb{R}^{n\times r} \right\}. \tag{4}$$

Especially, if $U = V$ and B is symmetric positive definite, then (4) reduces to

$$\Phi^\star := \min_{U} \left\{ \Phi(U) := (1/2)\|UU^T - B\|_F^2 : U \in \mathbb{R}^{n\times r} \right\}, \tag{5}$$

which was considered in [30]. Alternatively, if we choose $\Phi(U) := (1/2)\|\mathcal{A}(UU^T) - B\|_F^2$ in (2), then (1) reduces to the case studied in [2]. While both special cases, (4) and (5), possess a closed form solution via a truncated SVD and an eigenvalue decomposition, respectively, Gauss-Newton methods can also be applied to solve these problems. In [30], the authors demonstrated the advantages of a Gauss-Newton method for solving (5) via several encouraging numerical examples.

1.2 Related work

Low-rankness is key to recast many existing problems into new frameworks or to design new models with the aid of regularizers to promote solution structures in concrete applications including matrix completion (MC) [10], robust principle component analysis (RPCA) [9] and their variants. So far, extensions to group structured sparsity, low-rankness, tree models and tensor representation have attracted a great attention, see, e.g., [15,20,22,26,34,36,42]. A majority of research for low-rank models focusses on estimating sample complexity results for specific instances of (1), while various recent papers revolve around the RPCA settings, matrix completion, and their extensions [9,10,24]. Simple convex models originating from (1) have several advantages for designing solution methods, they unfortunately do not capture well the original model. Trading-off these two ingredients is key to achieve appropriate models for practical purposes.

Along with problem modeling, solution algorithms for (1) are a core step for solving practical problems in low-rank matrix completion and recovery. From an optimization-based viewpoint, we observe that existing methods for (1) either focus on specific applications or are limited to some classes of problems, where advanced computational techniques can be exploited. Among many others, convex optimization is perhaps one of the most powerful tools to solve several instances of (1) including MC, RPCA and their variants and extensions. Unfortunately, convex models only provide an approximation to the low-rank model (1) by convex relaxations using, e.g., nuclear or max norms, which may not adequately approximate the desired rank. Alternatively, nonconvex as well as discrete optimization methods have also been considered for solving (1), see, e.g., [6,27,29,35,40,41]. While these approaches work directly on the original problem (1), they can only find a local optimum or a critical point, and strongly depend on the priori knowledge of problems, the initial points of algorithms, and a predicted ranks. However, several empirical evidence have been provided to support these approaches, and surprisingly, in many cases, they outperform convex optimization approaches in terms of "accuracy" to the original model, and the overall computational time [27,29, 40]. Other approaches such as stochastic gradient descent, Riemann manifold descent, greedy methods, parallel and distributed algorithms have also been studied recently, see, e.g., [4,24,25,38,41].

1.3 Motivation and contributions

Optimization researchers have observed that Gauss-Newton (GN) methods work extremely well for nonlinear least-square problems [3]. Within the quadratic objective ϕ, when the residual term $\mathcal{A}(UV^T) - B$ in (1) is small or zero at solutions, GN methods can achieve local superlinear and even quadratic convergence rate. With a "good" initial guess (i.e., close to the solution set), GN methods often reach a stationary point within few iterations [13]. In many practical problems, we can often predict a "good" initial point using priori knowledge of our problem and underlying algorithm (e.g., steady states of dynamical systems, or previous iterations of algorithms) as a warm-start.

As in classical GN methods, we design an iterative scheme for solving (1) based on the linearization of the residual term $\mathcal{A}(UV^T) - B$ and the quadratic surrogate of ϕ. At each iteration, it requires to solve a simple convex problem to form a GN search direction and then incorporates with a globalization strategy to update the next iteration. In our setting, computing GN search direction reduces to solving a

linear least-squares problem, which is similar to alternating direction method (ADM) [40]. While ADM alternatively solves for each U and V, GN simultaneously solves for U and V using the linearization of UV^T. We have experienced that (*cf.* Subsection 7.1) GN uses a linearization of UV^T providing a good local approximate model to UV^T compared to the alternating form $U\bar{V}^T$ (or $\bar{U}V^T$), when $U-\bar{U}$ (or $V-\bar{V}$) is relatively large. This makes ADM saturated and does not significantly improve the objective values. In addition, without regularization, ADM may fail to converge as a counterexample in [19]. Moreover, ADM is not applicable to solve the symmetric case of (1), where we have $U = V$ without reformulation or introducing lifting variables, but the GN method is.

While Gauss-Newton methods have been widely used in nonlinear least squares [33], they are still mostly unexploited for matrix nonlinear optimization. Our aim in this paper is to extend the GN method for solving a class of problems (1) to the two aspects: general convex objective ϕ, and low-rank matrix variable settings. This work is also inspirited by a recent work in [30], where the authors considered a simple symmetric instance of (1), and demonstrated very encouraging numerical experiments via GN methods compared to other state-of-the-art algorithms.

Our contributions: Our specific contributions can be summarized as follows:

(a) We extend the Gauss-Newton method to solve low-rank matrix optimization problems of the form (1) involving general convex objective. We point out the existence of GN directions and provide their closed form formulation. We show empirically that our GN method achieve much higher accurate solutions compared to the common used alternating direction methods within the same number of iterations.

(b) We show that there exists an explicit step-size to guarantee a descent property of the Gauss-Newton direction. This allows us to perform a simple backtracking linesearch procedure to guarantee global convergence of the proposed method. We then specify our framework to the symmetric case with global convergence guarantee.

(c) We prove a local linear and quadratic convergence rate of the full-step Gauss-Newton variant under standard assumptions imposed on (1) at its solution set.

(d) Then, we develop a joint treatment between ADMM and the Gauss-Newton method to obtain a new algorithm for (1) that handles general objective ϕ. Under standard assumptions on (1), we prove global convergence of the proposed algorithm.

Unlike alternating direction methods whose only achieve sublinear convergence even with good initial points, GN methods may slightly require additional computation for GN directions, but they can achieve a fast local linear or quadratic convergence rate, which is key for online and real-time implementations. Alternatively, gradient descent-based methods can achieve local linear convergence but often require much strong assumptions imposed on (1). In contrast, GN methods work for "small residual" settings under mild assumptions, and can easily achieve high accuracy solutions.

1.4 Outline of the paper

The rest of this paper is organized as follows. We first review basic concepts related to problem (1) in Section 2. Section 3 presents a linesearch Gauss-Newton method for solving (1) and proves its convergence properties. Section 4 designs a Gauss-Newton ADMM algorithm for solving (1) and investigates its global convergence. Section 5 specifies the GN algorithm to the symmetric case and proves its convergence. Section 6 discusses the implementation aspects of our algorithms and their extension to

nonsmooth objective function. Numerical experiments are conducted in Section 7 with several applications in different fields. For clarity of presentation, we move all the proofs in the main text to the appendix.

2 Basic notations and optimality condition

We briefly state some basic notations, the optimality condition for (1), and the fundamental assumption.

2.1 Basic notation and concepts

For a matrix X, $\sigma_{\min}(X)$ and $\sigma_{\max}(X)$ denote its positive smallest and largest singular values, respectively. If X is symmetric, then $\lambda_{\min}(X)$ and $\lambda_{\max}(X)$ denote its smallest and largest eigenvalues, respectively. We use $X = P\Sigma Q^T$ for SVD and $X = U\Lambda U^{-1}$ for eigenvalue decomposition.

We denote by $X^\dagger$ the Moore-Penrose pseudo-inverse of X, i.e., $X^\dagger = (X^TX)^{-1}X^T$ when X has full-column rank. We also define $P_X := X(X^TX)^{-1}X^T \equiv XX^\dagger$ the projection onto the range space of X, and $P_X^\perp := \mathbb{I} - P_X$ the orthogonal projection of P_X, i.e., $P_XP_X^\perp = P_X^\perp P_X = 0$, where $\mathbb{I}$ is an identity. Clearly, $P_X^\perp X = 0$.

For a matrix X, we define $\mathrm{vec}\,(X) = (X_{11}, \cdots X_{m1}, \cdots, X_{1n}, \cdots, X_{mn})^T$ the vectorization of X. Given the vec operator, we define mat the inverse of vec such that $\mathrm{mat}\,(\mathrm{vec}\,(X)) = X$. For two matrices X and Y, $X \otimes Y$ denotes the Kronecker product of X and Y. We always have $\mathrm{vec}\,(AXB) = (B^T \otimes A)\mathrm{vec}\,(X)$ and $(A \otimes B)(C \otimes D) = AC \otimes BD$. For a linear operator $\mathcal{A}$, $\mathcal{A}^*$ denotes its adjoint operator.

2.2 Optimality condition and fundamental assumptions

We define $X := [U, V]$ as a joint variable of U and V in (1). First, we assume that ϕ in (1) is smooth. Then, the *optimality condition* of (1) can be written as follows:

$$\begin{cases} U_\star^T\mathcal{A}^*\left(\nabla\phi(\mathcal{A}(U_\star V_\star^T) - B)\right) = 0, \\ \mathcal{A}^*\left(\nabla\phi(\mathcal{A}(U_\star V_\star^T) - B)\right)V_\star \ = 0. \end{cases} \tag{6}$$

Any $X_\star = [U_\star, V_\star]$ satisfying (6) is called a *stationary point* of (1). We denote by $\mathcal{X}_\star$ the set of stationary points of (1). Since $r \le \min\{m, n\}$, the solution of (6) is generally nonunique. Our aim is to design algorithms for generating a sequence $\{X_k\}$ converging to $X_\star \in \mathcal{X}_\star$ relying on the following fundamental assumption.

Assumption A.21 *Problem* (1) *satisfies the following conditions:*

(a) ϕ *is* L_ϕ*-smooth and* μ_ϕ*-convex, i.e.,* $\nabla\phi$ *satisfies* (*with* $0 \le \mu_\phi \le L_\phi < +\infty$) *that*

$$\frac{\mu_\phi}{2} \le \phi(y) - \phi(x) - \langle\nabla\phi(x), y - x\rangle \le \frac{L_\phi}{2}\|y - x\|_2^2, \quad \forall x, y \in \mathrm{dom}(\phi). \tag{7}$$

(b) *The set of stationary points of* (1) *is nonempty.*

If $\nabla\phi$ is Lipschitz continuous with the Lipschitz constant L_ϕ, then (7) holds [32]. We allow $\mu_\phi = 0$, which also covers the non-strongly convex case. Since ϕ is smooth and $\mathcal{A}$ is linear, Φ is also smooth. In addition, Assumption A.21(a) covers a wide range of applications including logistic loss, Huber loss and entropy in nonlinear regression and machine learning [5].

3 Line-search Gauss-Newton method

We develop here a linesearch Gauss-Newton (Ls-GN) algorithm for solving (1) which has convergence guarantee.

3.1 Forming a surrogate of the objective

By Assumption A.21, it follows from (7) and $\Phi(U,V) := \phi(\mathcal{A}(UV^T) - B)$ that

$$\Phi(\hat{U},\hat{V}) \le \Phi(U,V) + \frac{L}{2}\|\hat{U}\hat{V}^T - (UV^T - L^{-1}\Phi'(UV^T))\|_F^2 - \frac{1}{2L}\|\Phi'(UV^T)\|_F^2, \quad (8)$$

for any U, V, $\hat{U}$, and $\hat{V}$, where $\Phi'(UV^T) := \mathcal{A}^*\nabla\phi(\mathcal{A}(UV^T) - B)$ is the gradient of Φ, and $L := L_\phi\|\mathcal{A}\|^2$ is the Lipschitz constant of the gradient of $\phi(\mathcal{A}(\cdot) - B)$.

Descent optimization methods rely on finding a descent direction of Φ by approximately minimizing the right-hand side surrogate of Φ in (8). Unfortunately, this surrogate remains nonconvex due to the bilinear term $\hat{U}\hat{V}^T$. Our next step is to linearize this bilinear term around a given point $[U,V]$ as follows:

$$\hat{U}\hat{V}^T \approx UV^T + U(\hat{V} - V)^T + (\hat{U} - U)V^T. \quad (9)$$

Then, the minimization of the right-hand side surrogate (8) is approximated by

$$\min_{\hat{U},\hat{V}} \left\{ (1/2)\|U(\hat{V} - V)^T + (\hat{U} - U)V^T + L^{-1}\Phi'(UV^T)\|_F^2 \right\}. \quad (10)$$

This problem is a linear least-squares, and can be solved by standard linear algebra.

3.2 Computing Gauss-Newton direction

Let $D_U := \hat{U} - U$, $D_V := \hat{V} - V$ and $Z := -L^{-1}\mathcal{A}^*\Big(\nabla\phi(\mathcal{A}(UV^T) - B)\Big)$. Then, we rewrite (10) as

$$\min_{D_U, D_V} \left\{ (1/2)\|UD_V^T + D_U V^T - Z\|_F^2 : D_U \in \mathbb{R}^{m\times r}, D_V \in \mathbb{R}^{m\times r} \right\}. \quad (11)$$

The optimality condition of (11) becomes

$$\begin{cases} U^T U D_V^T + U^T D_U V^T &= U^T Z, \\ U D_V^T V + D_U V^T V &= ZV. \end{cases} \quad (12)$$

As usual, we can refer to (12) as the normal equation of (11). We show in Lemma 1 a closed form solution of (12), whose proof is in Appendix A.1.

Lemma 1 *The rank of the square linear system* (12) *does not exceed* $r(m+n-r)$. *In addition,* (12) *has solution. If* $\mathrm{rank}\,(U) = \mathrm{rank}\,(V) = r \le \min\{m,n\}$, *then the solution of* (12) *is given explicitly by*

$$\begin{cases} D_U &= P_U^\perp Z(V^\dagger)^T + U\hat{D}_r, \\ D_V^T &= U^\dagger Z - \hat{D}_r V^T. \end{cases} \quad (13)$$

which forms a linear subspace in $\mathbb{R}^{r\times r}$, *where* $U^\dagger$ *and* $V^\dagger$ *are the Moore-Penrose pseudo inverses of* U *and* V, *respectively, and* $\hat{D}_r \in \mathbb{R}^{r\times r}$ *is an arbitrary matrix.*

In particular, if we choose $\hat{D}_r := 0.5U^\dagger Z(V^\dagger)^T \in \mathbb{R}^{r\times r}$, *then*

$$D_U = \big(\mathbb{I}_m - 0.5P_U\big)Z(V^\dagger)^T \quad \text{and} \quad D_V^T = U^\dagger Z\big(\mathbb{I}_n - 0.5P_V\big). \quad (14)$$

Moreover, the optimal value of (11) *is* $(1/2)\|P_U^\perp Z P_V^\perp\|_F^2$.

Lemma 1 also shows that if either Z is in the null space of P_U or Z^T is in the null space of P_V, then $\|P_U^{\perp} Z P_V^{\perp}\|_F^2 = 0$. We note that (14) only gives us one choice for $D_X := [D_U, D_V]$. We can choose $\hat{D}_r = \mathbf{0}^r$ to obtain a simple GN search direction.

Remark 1 Let $m = n$. If we assume that $U = V$, then $D_U = D_V$ and

$$D_U = P_U^{\perp} Z (U^{\dagger})^T + U\hat{D}_r, \text{ where } \hat{D}_r \in \mathcal{S}_r := \left\{ \hat{D}_r \in \mathbb{R}^{r\times r} : \hat{D}_r + \hat{D}_r^T = U^{\dagger} Z (U^{\dagger})^T \right\}.$$

Clearly, $\mathcal{S}_r$ is a linear subspace, and its dimension is $r(r+1)/2$.

3.3 The damped-step Gauss-Newton scheme

Using Lemma 1, we can form a damped step Gauss-Newton scheme as follows:

$$\begin{cases} U_+ := U + \alpha D_U, \\ V_+ := V + \alpha D_V, \end{cases} \tag{15}$$

where D_U and D_V defined in (14) is the Gauss-Newton direction, and $\alpha > 0$ is a given step-size determined in the next lemma.

Since the GN direction computed by solving (11) is not unique, we need to choose an appropriate D_X such that this direction is a descent direction of Φ at X. We prove in the following lemma that the GN direction computed by (14) is indeed a descent direction of Φ at X. The proof of this lemma is given in Appendix A.2.

Lemma 2 *Let $X := [U, V]$ be a non-stationary point of (1) and $D_X := [D_U, D_V]$ be computed by (14). If $D_X \neq 0$ and α is chosen such that $0 < \alpha \leq \underline{\alpha}$ with*

$$\underline{\alpha} := \min\left\{1, \frac{L\sigma_{\min}^3}{2\|\nabla\Phi(U,V)\|_F}, \frac{3\sigma_{\min}^4}{32\sigma_{\max}^2\|\Phi'(UV^T)\|_F}\right\} \in (0,1], \tag{16}$$

then we have

$$\Phi(U_+, V_+) \leq \Phi(U,V) - \frac{\alpha\sigma_{\min}^2}{128L\sigma_{\max}^4}\|\nabla\Phi(U,V)\|^2, \tag{17}$$

where $\Phi'(\cdot) = \mathcal{A}^*\nabla\phi(\mathcal{A}(\cdot) - B)$, $L := L_\phi \|\mathcal{A}\|^2$, $\sigma_{\min} := \min\{\sigma_{\min}(U), \sigma_{\min}(V)\}$, and $\sigma_{\max} := \max\{\sigma_{\max}(U), \sigma_{\max}(V)\}$. Consequently, D_X is a descent direction of Φ.

Lemma 2 shows that if the residual term $\mathcal{A}^*\nabla\phi(\mathcal{A}(UV^T) - B)$ is sufficient small near $\mathcal{X}_\star$, then we obtain full-step $\alpha = 1$ since both $\Phi'(UV^T)$ and $\nabla\Phi(UV^T)$ are small.

The existence of the GN direction in Lemma 1 requires U and V to be full-rank. This condition is shown in the following lemma whose proof is in Appendix A.3.

Lemma 3 *If $\operatorname{rank}(U) = \operatorname{rank}(V) = r$, then $X_+ := [U_+, V_+]$ updated by (15) using the step-size $\underline{\alpha}$ in (16) satisfies*

$$\sigma_{\min}(U_+) \geq 0.5\sigma_{\min}(U) \quad \text{and} \quad \sigma_{\min}(V_+) \geq 0.5\sigma_{\min}(V). \tag{18}$$

Hence, (15) preserves the rank of U_+ and V_+, i.e., $\operatorname{rank}(U_+) = \operatorname{rank}(V_+) = r$.

3.4 The algorithm and its global convergence

Theoretically, we can use the step-size $\underline{\alpha}$ in Lemma 2 for (15). However, in practice, computing $\underline{\alpha}$ requires a high computational intensity. We instead incorporate the GN scheme (15) with an Armijo's backtracking linesearch to find an appropriate step-size $\alpha \geq \beta\underline{\alpha}$ for given $\beta \in (0,1)$.

Given $\alpha_0 > 0$, find the smallest number $i_k \geq 0$ such that $\alpha := \beta^{i_k}\alpha_0 \geq \underline{\alpha}$ and

$$\Phi(U + \alpha D_U, V + \alpha D_V) \leq \Phi(U, V) - 0.5c_1\alpha\|\nabla\Phi(U, V)\|_F^2, \tag{19}$$

where $c_1 > 0$ and $\beta \in (0, 1)$ are given (e.g., $c_1 = 0.5$ and $\beta := (\sqrt{5}–1)/(\sqrt{5}+1)$).

By Lemma 2, this linesearch procedure is terminated after finite iterations i_k:

$$i_k \leq \lfloor \log_\beta(\underline{\alpha}/\alpha_0)\rfloor + 1, \tag{20}$$

where $\underline{\alpha}$ is given by (16). Now, we present the complete linesearch Gauss-Newton algorithm for solving (1) as in Algorithm 1.

Algorithm 1 (*Linesearch Gauss-Newton algorithm* (Ls-GN))

1: **Initialization:**
2: Given a tolerance $\varepsilon > 0$. Choose $X_0 := [U_0, V_0]$. Set $c_1 := 0.5$ and $\alpha_0 := 1$.
3: **for** $k = 0$ **to** $k_{\max}$ **do**
4: *GN direction*: Let $Z_k := -L^{-1}\Phi'(U_kV_k^T)$. Compute $D_{X_k} := [D_{U_k}, D_{V_k}]$:

$$D_{U_k} := \left(\mathbb{I}_m - 0.5P_{U_k}\right) Z_k(V_k^\dagger)^T \quad \text{and} \quad D_{V_k} = \left(\mathbb{I}_n - 0.5P_{V_k}\right) Z_k^T(U_k^\dagger)^T.$$

5: *Stopping criterion*: If `stopping_criterion`, then TERMINATE.
6: *Backtracking linesearch*: Find the smallest number $i_k \geq 0$ such that

$$\Phi(U_k + \alpha_0\beta^{i_k}D_{U_k}, V_k + \alpha_0 2^{-i_k}D_{V_k}) \leq \Phi(U_k, V_k) - 0.5c_1\alpha_0\beta^{i_k}\|\nabla\Phi(U_k, V_k)\|_F^2.$$

Set $\alpha_k := \alpha_0\beta^{i_k}$.
7: Update $X_{k+1} := [U_{k+1}, V_{k+1}]$ as $U_{k+1} := U_k + \alpha_k D_{U_k}$ and $V_{k+1} := V_k + \alpha_k D_{V_k}$.
8: **end for**

Complexity-per-iteration: The main steps of Algorithm 1 are Steps 4 and 6, where we need to compute D_{X_k} and perform the linesearch routine, respectively.

(a) We can show that computing D_{X_k} requires two inverses $(U^TU)^{-1}$ and $(V^TV)^{-1}$ of the size $r \times r$, and two matrix-matrix multiplications (of the size $m \times r$ or $n \times r$).

(b) Evaluating Φ' requires one matrix-matrix multiplication UV^T and one evaluation $\mathcal{A}^*\nabla\phi(\mathcal{A}(\cdot) - B)$. When $\mathcal{A}$ is a subset projection $\mathcal{P}_\Omega$ (e.g., in matrix completion), we can compute $(UV^T)_{(i,j)\in\Omega}$ instead of the full matrix UV^T.

(c) Each step of the linesearch needs one matrix-matrix multiplication UV^T and one evaluation of Φ. It requires at most $\lfloor \log_\beta(\underline{\alpha}/\alpha_0)\rfloor + 1$ linesearch iterations. However, we observe from numerical experiments that i_k often varies from 1 to 2 on average.

Global convergence: Since (1) is nonconvex, we only expect $\{X_k\}$ generated by Algorithm 1 to converge to a stationary point $X_\star \in \mathcal{X}_\star$. However, Lemma 3 only guarantees the full-rankness of U_k and V_k at each iteration, but we may have $\lim_{k\to\infty}\sigma_{\min}(U_k) = 0$ or $\lim_{k\to\infty}\sigma_{\min}(V_k) = 0$. In order to prove a global convergence of Algorithm 1, we require one additional condition: There exists $\underline{\sigma} > 0$ such that:

$$\sigma_{\min}(U_k) \geq \underline{\sigma} \quad \text{and} \quad \sigma_{\min}(V_k) \geq \underline{\sigma} \quad \text{for all } k \geq 0. \tag{21}$$

Under Assumption A.21, the following sublevel set of Φ is bounded for given $\gamma > 0$:

$$\mathcal{L}_\Phi(\gamma) := \{[U, V] \in \mathrm{dom}(\Phi) : \Phi(U, V) \leq \gamma\}.$$

We prove in Appendix A.4 a global convergence of Algorithm 1 stated as follows.

Theorem 1 *Let $\{X_k\}$ with $X_k := [U_k, V_k]$ be the sequence generated by Algorithm 1. Then, under Assumption A.21, we have*

$$\sum_{k=0}^{\infty} \alpha_k \|\nabla \Phi(U_k, V_k)\|_F^2 < +\infty, \quad \text{and} \quad \lim_{k\to\infty} \alpha_k \|\nabla \Phi(U_k, V_k)\|_F = 0. \tag{22}$$

If, in addition, the condition (21) *holds and $\{X_k\}$ is bounded, then*

$$\lim_{k\to\infty} \|\nabla \Phi(U_k, V_k)\|_F = 0. \tag{23}$$

There exists a limit point $X_\star$ of $\{X_k\}$, and any limit point $X_\star$ is in $\mathcal{X}_\star$.

3.5 Local linear convergence without strong convexity

We prove a local convergence of the full-step Gauss-Newton scheme (15) when $\alpha = 1$. Generally, problem (1) does not satisfy the regularity assumption: Jacobian $J_R(X) = A[V \otimes \mathbb{I}_m, \mathbb{I}_n \otimes U] \in \mathbb{R}^{l\times(m+n)r}$ of the objective residual $R(X) := \mathcal{A}(UV^T) - B$ in (1) is not full-column rank, where A is the matrix form of the linear operator $\mathcal{A}$. However, we can still guarantee a fast local convergence under the following conditions:

Assumption A.31 *Problem* (1) *satisfies the following conditions:*

(a) *ϕ is twice differentiable on a neighborhood $\mathcal{N}(Z_\star)$ of $Z_\star = \mathcal{A}(U_\star V_\star^T) - B$, and its Hessian $\nabla^2\phi$ is Lipschitz continuous in $\mathcal{N}(Z_\star)$ with the constant $L_{\phi''} > 0$.*

(b) *The Hessian $\nabla^2\Phi(X_\star)$ of $\Phi(X) := \phi(\mathcal{A}(UV^T) - B)$ at $X_\star \in \mathcal{X}_\star$ satisfies*

$$\| \left[\mathbb{I} - L^{-1} H(X)^\dagger \nabla^2 \Phi(X_\star)\right](X - X_\star)\|_F \le \kappa(X_\star)\|X - X_\star\|_F, \quad \forall X \in \mathcal{N}(X_\star), \tag{24}$$

where $H(X) := \begin{bmatrix} V^T \otimes U & V^T V \otimes \mathbb{I}_m \\ \mathbb{I}_n \otimes U^T U & V \otimes U^T \end{bmatrix}$, $L := L_\phi \|\mathcal{A}\|^2$, *and* $0 \le \kappa(X_\star) \le \bar{\kappa} < 1$.

Assumption A.31(b) relates to a "small residual condition". For instance, if $\phi(\cdot) = (1/2)\|\cdot\|_2^2$, and $\mathcal{A} = \mathbb{I}$, the identity operator, then the residual term becomes $R(X) = UV^T - B$, and the objective Φ is $\Phi(X) = (1/2)\|R(X)\|_F^2$. In this case, condition (24) holds if $\|R(X_\star)\|_F \le \kappa(X_\star) < 1$ (i.e., we have a "small residual" case).

Now, we prove in Appendix A.7 local convergence of the full-step variant of (15).

Theorem 2 *Let $\{X_k\}$ with $X_k := [U_k, V_k]$ be the sequence generated by* (15) *with step-size $\alpha_k = 1$, and $X_\star := [U_\star, V_\star] \in \mathcal{X}_\star$ be a given stationary point of* (1) *such that* $\operatorname{rank}(U_\star) = \operatorname{rank}(V_\star) = r$. *Assume that Assumptions A.21 and A.31 hold. Then, there exists a neighborhood $\mathcal{N}(X_\star)$ of $X_\star$ and a constant $K_1 > 0$ such that*

$$\|X_{k+1} - X_\star\|_F \le \big(\bar{\kappa} + 0.5K_1\|X_k - X_\star\|_F\big)\|X_k - X_\star\|_F, \quad \forall X_k \in \mathcal{N}(X_\star). \tag{25}$$

Consequently, if $H(X_\star)^\dagger \nabla^2\Phi(X_\star) = L\mathbb{I}$ in (24) (*i.e., zero residual*), *then there exists a constant $K_2 > K_1$ such that $\{X_k\}$ starting from $X_0 \in \mathcal{N}(X_\star)$ such that $\|X_0 - X_\star\|_F < 2K_2^{-1}$ converges quadratically to $X_\star \in \mathcal{X}_\star$.*

If $\kappa(X_\star) \in (0, 1)$ in (24) (*i.e., small residual*), *then, for any $X_0 \in \mathcal{N}(X_\star)$ such that $\|X_0 - X_\star\|_F \le \bar{r}_0 < 2K_1^{-1}(1 - \bar{\kappa})$, $\{X_k\}$ converges to $X_\star$ at a linear rate.*

4 Gauss-Newton alternating direction method of multipliers

The GN method only works well and has a fast local convergence for the "small residual" case. In general, it may converge very slowly or even fails to converge. In this section, we propose to combine the GN scheme (15) and the alternating direction method of multipliers (ADMM) to develop a new algorithm for solving (1) called GN-ADMM. The main steps of this algorithm are described below.

4.1 The augmented Lagrangian and ADMM scheme

We introduce a slack variable $W = \mathcal{A}(UV^T) - B$ and rewrite (1) as the following constrained problem:

$$\Phi_\star := \min_{U,V,W} \left\{ \phi(W) \ : \ \mathcal{A}(UV^T) - W = B \right\}. \tag{26}$$

We can define the augmented Lagrangian function associated with (26) as

$$\begin{aligned} \mathcal{L}_\rho(U,V,W,\Lambda) &:= \phi(W) + \langle \Lambda, \mathcal{A}(UV^T) - W - B\rangle + (\rho/2)\|\mathcal{A}(UV^T) - W - B\|_2^2 \\ &= \phi(W) + (\rho/2)\|\mathcal{A}(UV^T) - W - B + \rho^{-1}\Lambda\|_2^2 - (1/(2\rho))\|\Lambda\|_2^2, \end{aligned} \tag{27}$$

where $\rho > 0$ is a penalty parameter and Λ is the corresponding Lagrange multiplier.

Next, we apply the standard ADMM scheme to (26) which leads to 3 steps:

$$(U_{k+1}, V_{k+1}) := \operatorname*{argmin}_{U,V} \left\{ \|\mathcal{A}(UV^T) - W_k - B + \rho^{-1}\Lambda_k\|_2^2 \right\}, \tag{28a}$$

$$W_{k+1} := \operatorname*{argmin}_{W} \left\{ \phi(W) + (\rho/2)\|W - \left(\mathcal{A}(U_{k+1}V_{k+1}^T) - B + \rho^{-1}\Lambda_k\right)\|_2^2 \right\}, \tag{28b}$$

$$\Lambda_{k+1} := \Lambda_k + \rho(\mathcal{A}(U_{k+1}V_{k+1}^T) - W_{k+1} - B). \tag{28c}$$

Obviously, both subproblems (28a) and (28b) remain computationally intensive. While (28a) is nonconvex, (28b) is smooth and convex. Without any further step applying to (28), convergence theory for this nonconvex ADMM scheme can be found in several recent papers including [28,39,40]. However, (28) remains impractical since (28a) and (28b) cannot be solved with a closed form or highly accurate solution. Our next step is to approximately solve these two subproblems.

4.2 Approximation of the alternating steps

Gauss-Newton step for the UV-subproblem (28a)*:* We first apply on step of the GN scheme (15) to solve (28a) as follows. We first approximate $\|\mathcal{A}(UV^T) - W_k - B + \rho^{-1}\Lambda_k\|_2^2$ by using the quadratic upper bound of $\mathcal{A}(\cdot)$ and the linearization $U_kV_k^T + U_kD_V^T + D_UV_k^T$ of UV^T with $D_U := U - U_k$ and $D_V := V - V_k$. By letting $Z_k := -L_{\mathcal{A}}^{-1}\mathcal{A}^*\left(\mathcal{A}(U_kV_k^T) - W_k - B + \rho^{-1}\Lambda_k\right)$ with $L_{\mathcal{A}} := \|\mathcal{A}\|^2$, we solve

$$[D_{U_k}, D_{V_k}] := \operatorname*{argmin}_{D_U, D_V} \left\{ \mathcal{Q}_k(D_U, D_V) := \frac{1}{2}\|U_kD_V^T + D_UV_k^T - Z_k\|_F^2 \right\}. \tag{29}$$

Here, the Lipschitz constant $L_{\mathcal{A}} := \|\mathcal{A}\|^2$ can be computed by a power method [17]. Using Lemma 1, we can compute $[D_{U_k}, D_{V_k}]$ as

$$\begin{cases} D_{U_k} &= \left(\mathbb{I}_m - 0.5P_{U_k}\right)Z_k(V_k^\dagger)^T \\ D_{V_k}^T &= U_k^\dagger Z_k\left(\mathbb{I}_n - 0.5P_{V_k}\right). \end{cases} \tag{30}$$

The corresponding objective value is $\mathcal{Q}_k(D_{U_k}, D_{V_k}) := (1/2)\|P_{u_k}^{\perp} Z_k P_{V_k}^{\perp}\|_F^2$. Then, we update $X_{k+1} := [U_{k+1}, V_{k+1}]$ as

$$U_{k+1} := U_k + \alpha_k D_{U_k} \quad \text{and} \quad V_{k+1} := V_k + \alpha_k D_{V_k}, \tag{31}$$

where $\alpha_k > 0$ is a given step-size computed by a linesearch procedure as in (19).

Gradient step for the W-subproblem (28b)*:* If ϕ does not have tractable proximal operator, we approximate (28b) by using one gradient step as

$$W_{k+1} := \operatorname*{argmin}_{W} \Big\{ \frac{L_\phi}{2}\|W - (W_k - L_\phi^{-1}\nabla\phi(W_k))\|_2^2 + \frac{\rho}{2}\|W - E_k\|_2^2 \Big\}, \tag{32}$$

where $E_k := \mathcal{A}(U_{k+1}V_{k+1}^T) - B + \rho^{-1}\Lambda_k$. Solve (32) directly, we get

$$W_{k+1} := (\rho + L_\phi)^{-1}\left(L_\phi W_k - \nabla\phi(W_k) + (\Lambda_k + \rho(\mathcal{A}(U_{k+1}^T V_{k+1}) - B)\right). \tag{33}$$

4.3 The Gauss-Newton ADMM algorithm

By putting (31), (28c), and (28b) or (33) together, we obtain the following GN-ADMM scheme with two options:

$$\begin{cases} Z_k & := -L_{\mathcal{A}}^{-1}\mathcal{A}^*\left(\mathcal{A}(U_kV_k^T) - W_k - B + \rho^{-1}\Lambda_k\right), \\ U_{k+1} & := U_k + \alpha_k\big(\mathbb{I}_m - 0.5P_{U_k}\big)Z_k(V_k^\dagger)^T, \\ V_{k+1} & := V_k + \alpha_k\big(\mathbb{I}_n - 0.5P_{V_k}\big)Z_k(U_k^\dagger)^T, \\ W_{k+1} & \text{ is computed by (28b) for Option 1, or by (32) for Option 2,} \\ \Lambda_{k+1} & := \Lambda_k + \rho(\mathcal{A}(U_{k+1}V_{k+1}^T) - W_{k+1} - B). \end{cases} \tag{34}$$

Clearly, computing $[U_{k+1}, V_{k+1}]$ in (34) using the step-size in Lemma 2 is impractical. Similar to Algorithm 1, we find an appropriate α_k by a backtracking linesearch on $\mathcal{Q}_k(U,V) := (1/2)\left\|\mathcal{A}(UV^T) - W_k - B + \rho^{-1}\Lambda_k\right\|_2^2$ as

$$\mathcal{Q}(U_k + \alpha D_{U_k}, V_k + \alpha_k V_k) \le \mathcal{Q}(U_k, V_k) - 0.5c_1\alpha_k\Delta_k^2, \tag{35}$$

where $\Delta_k^2 := \|U_k^T\mathcal{A}^*(E_k - W_k)\|_F^2 + \|\mathcal{A}^*(E_k - W_k)V_k\|_F^2$ and $\alpha_k := \beta^{i_k}\alpha_0$ with $\alpha_0 > 0$ and $\beta := (\sqrt{5}-1)/(\sqrt{5}+1) \in (0,1)$ given a priori. Obviously, by Lemma 2, this linesearch procedure terminates after finite iterations i_k satisfying (20). In addition, $D_{X_k} := [D_{U_k}, D_{V_k}]$ is a descent direction of the quadratic objective $\mathcal{Q}_k$ at X_k. Finally, we expand (34) algorithmically as in Algorithm 2.

Complexity-per-iteration: The main steps of Algorithm 2 remain at Steps 4 and 5, where they require to compute $D_{X_k} := [D_{U_k}, D_{V_k}]$ and to perform a linesearch procedure, respectively. Steps 6 and 8 only require matrix-matrix additions which have the complexity of $\mathcal{O}(m \times n)$. Overall, the complexity per-iteration of Algorithm 2 is higher than of Algorithm 1, but as we can see from Section 7, we can simply use the full-step GN scheme at Step 4 without linesearch, and Algorithm 2 often requires fewer number of iterations than Algorithm 1. Moreover, Algorithm 2 seems working well for the "large residual case", i.e., $\mathcal{A}^*\nabla\phi(\mathcal{A}(U_\star V_\star^T) - B)$ is large.

Algorithm 2 (*Gauss-Newton ADMM algorithm* (GN-ADMM))

1: **Initialization:**
2: Given $\varepsilon > 0$, choose $\rho > 0$ and $X_0 := [U_0, V_0]$. Set $W_0 := U_0 V_0^T$ and $\Lambda_0 := \mathbf{0}^{m\times n}$.
3: **for** $k = 0$ **to** $k_{\max}$ **do**
4: *Gauss-Newton step*: Compute a GN direction $D_{X_k} := [D_{U_k}, D_{V_k}]$ by (30).
5: *Linesearch step*: Find $\alpha_k > 0$ from the linesearch condition (35) and update

$$U_{k+1} := U_k + \alpha_k D_{U_k} \quad \text{and} \quad V_{k+1} := V_k + \alpha_k D_{V_k}.$$

6: *Gradient step*: Evaluate $Y_{k+1} := \mathcal{A}(U_{k+1}V_{k+1}^T) - B$, and $\Phi'(W_k)$, and

Option 1: update W_{k+1} by (28b) **Option 2**: update W_{k+1} by (32)

7: If `stopping_criterion`, then TERMINATE.
8: Update $\Lambda_{k+1} := \Lambda_k + \rho(Y_{k+1} - W_{k+1})$.
9: **end for**

4.4 Global convergence analysis

We first write down the optimality condition (or KKT condition) for (26) as follows:

$$\nabla\phi(W_\star) - \mathcal{A}^*(\Lambda_\star) = 0,\ U_\star^T\mathcal{A}^*(\Lambda_\star) = 0,\ \mathcal{A}^*(\Lambda_\star)V_\star = 0, \text{ and } \mathcal{A}(U_\star V_\star^T) - W_\star = B. \tag{36}$$

This condition can be rewritten as (6) by eliminating $W_\star$ and the multiplier $\Lambda_\star$. Hence, if $[U_\star, V_\star, W_\star, \Lambda_\star]$ satisfies (36), then $X_\star := [U_\star, V_\star] \in \mathcal{X}_\star$.

The following lemma provides a key step to prove the convergence of Algorithm 2, whose proof is given in Appendix A.5.

Lemma 4 *Let $\{[U_k, V_k, W_k, \Lambda_k]\}$ be the sequence generated by Algorithm 2. Then, under Assumption A.21, the following statements hold:*

(a) *The sequence $\{[U_k, V_k, W_k]\}$ is bounded. In addition, for $k \geq 1$, we have*

$$\begin{aligned} \|\Lambda_{k+1} - \Lambda_k\|_2 &\leq L_\phi\|W_{k+1} - W_k\|_2 \qquad \textit{for } \textbf{\textit{Option 1}}, \\ \textit{or } \|\Lambda_{k+1} - \Lambda_k\|_2 &\leq L_\phi\big(\|W_k - W_{k-1}\|_2 + \|W_{k+1} - W_{k-1}\|_2\big) \textit{for } \textbf{\textit{Option 2}}. \end{aligned} \tag{37}$$

(b) *Let $\mathcal{L}_\rho$ defined by* (27)*, then, for any $\rho > 0$, we have*

$$\begin{aligned} \mathcal{L}_\rho(U_{k+1}, V_{k+1}, W_{k+1}, \Lambda_{k+1}) \leq \mathcal{L}_\rho(U_k, V_k, W_k, \Lambda_k) &- \frac{\eta_1}{2}\|W_{k+1} - W_k\|_2^2 + \frac{\eta_0}{2}\|W_k - W_{k-1}\|_2^2 \\ &- \frac{c_1\rho\alpha_k}{2}\left[\|U_k^T\mathcal{A}^*(E_k - W_k)\|_F^2 + \|\mathcal{A}^*(E_k - W_k)V_k\|_F^2\right], \end{aligned} \tag{38}$$

where $E_k := \mathcal{A}(U_k V_k^T) - B + \rho^{-1}\Lambda_k$, and

$$\begin{aligned} \eta_1 &:= \rho^{-1}\big(\rho^2 + \mu_\phi\rho - 2L_\phi^2\big) \quad \textit{and } \eta_0 := 0 \qquad \textit{for } \textbf{\textit{Option 1}}, \\ \textit{or } \ \eta_1 &:= \rho^{-1}\big(\rho^2 + L_\phi\rho - 4L_\phi^2\big) \quad \textit{and } \eta_0 := 8\rho^{-1}L_\phi^2 \textit{ for } \textbf{\textit{Option 2}}. \end{aligned} \tag{39}$$

Similar to Algorithm 1, we prove a global convergence of Algorithm 2 in the following theorem, whose proof is deferred to Appendix A.6.

Theorem 3 *Under Assumption A.21 and the rank condition* (21)*, let* $\{[U_k, V_k]\}$ *be the sequence generated by Algorithm 2 be bounded. Then, if we choose* ρ *such that*

$$\begin{cases} \rho > 0.5\big(\big(\mu_\phi + 8L_\phi^2\big)^{1/2} + \mu_\phi\big) & \text{for } \textbf{\textit{Option 1}}, \\ \rho > 3L_\phi & \text{for } \textbf{\textit{Option 2}}, \end{cases} \tag{40}$$

then

$$\lim_{k\to\infty} \|\nabla\Phi(U_k, V_k)\|_F = 0. \tag{41}$$

Consequently, there exists a limit point $X_\star := [U_\star, V_\star]$ *of* $\{[U_k, V_k]\}$*, and* $X_\star \in \mathcal{X}_\star$*.*

Remark 2 We note that our results in Lemma 4 and Theorem 3 can be extended to a regularized alternating direction ADMM (shortly, RAD-ADMM) algorithm for solving (26) by substituting the Gauss-Newton step at Step 4 of Algorithm 2 by the following regularized alternating direction step:

$$\begin{cases} U_{k+1} := \mathop{\mathrm{argmin}}_U \left\{ (1/2)\|UV_k^T - Z_k\|_F^2 + (\gamma_u/2)\|U - U_k\|_F^2 \right\}, \\ V_{k+1} := \mathop{\mathrm{argmin}}_V \left\{ (1/2)\|U_{k+1}V^T - Z_k\|_F^2 + (\gamma_v/2)\|V - V_k\|_F^2 \right\}, \end{cases} \tag{42}$$

where Z_k is given in (29), $\gamma_u > 0$ and $\gamma_v > 0$ are two given regularization parameters. Then, using $\mathcal{Q}_k$ in (35), we can easily prove that

$$\mathcal{Q}_k(U_{k+1}, V_{k+1}) \le \mathcal{Q}_k(U_k, V_k) - \tfrac{L_{\mathcal{A}}\gamma_u}{2}\|U_{k+1} - U_k\|_F^2 - \tfrac{L_{\mathcal{A}}\gamma_v}{2}\|V_{k+1} - V_k\|_F^2.$$

With similar proofs as in Lemma 4, we can show a global convergence of Algorithm 2 with Step 4 being replaced by (42) as in Theorem 3. We omit the details here.

5 Symmetric low-rank matrix optimization

We can develop a symmetric GN algorithm for solving the following special symmetric setting of (1) when $U = V$:

$$\Phi^\star := \min_U \left\{ \Phi(U) := \phi\left(\mathcal{A}(UU^T) - B\right) : U \in \mathbb{R}^{m\times r} \right\}. \tag{43}$$

We emphasize that (21) is a generalization of the least-squares problem considered in [30]. In addition, we cannot directly apply alternating trick in Remark 2 to (43) without reformulating the problem. The optimality condition of (43) is written as

$$U^T\mathcal{A}^*\left(\nabla\phi(\mathcal{A}(UU^T) - B)\right) = 0. \tag{44}$$

Any point $U_\star$ satisfying this condition is called a *stationary point* of (43). Similar to Assumption A.21, we assume that the set of stationary point $\mathcal{U}_\star$ of (43) is nonempty.

We now customize Algorithm 1 to find a stationary point of (43). First, since $U = V$, the symmetric Gauss-Newton direction can be computed from Remark 1 as

$$D_U = (\mathbb{I} - 0.5P_U)\, Z(U^\dagger)^T, \text{ where } Z = -L^{-1}\Phi'(UU^T) \equiv -L^{-1}\mathcal{A}^*\left(\nabla\phi(\mathcal{A}(UU^T) - B)\right).$$

Combining this step and modifying the linesearch procedure (19) we can describe a new variant of Algorithm 1 for solving (43) as in Algorithm 3.

Algorithm 3 (*Symmetric linesearch Gauss-Newton algorithm* (SLs-GN))

1: **Initialization:**
2: Given a tolerance $\varepsilon > 0$. Choose $U_0 \in \mathbb{R}^{m\times r}$. Set $\alpha_0 := 1$ and $c_1 := 0.5$.
3: **for** $k = 0$ **to** $k_{\max}$ **do**
4: *Gauss-Newton step*: Evaluate $Z_k := -L^{-1}\mathcal{A}^*\nabla\phi(\mathcal{A}(U_kU_k^T) - B)$ and compute

$$D_{U_k} := \left(\mathbb{I}_m - 0.5P_{U_k}\right) Z_k(U_k^\dagger)^T.$$

5: If $\|D_{U_k}\|_F \le \varepsilon\max\{1, \|U_k\|_F\}$, then TERMINATE.
6: *Linesearch*: Find the smallest number $i_k \ge 0$ such that $\alpha_{i_k} := \beta^{i_k}\alpha_0$ and

$$\Phi(U_k + \alpha_{i_k}D_{U_k}) \le \Phi(U_k) - 0.5c_1\alpha_{i_k}\|\nabla\Phi(U_k)\|_F^2.$$

7: Update the new point: $U_{k+1} := U_k + \alpha_k D_{U_k}$.
8: **end for**

Complexity-per-iteration: Computing $U^\dagger$ requires one QR-factorization of an $m \times r$ matrix to get $[Q, R] = \mathtt{qr}(U)$. Then, we form $U^\dagger = R^\dagger Q^T$, where $R^\dagger$ is obtained by solving an upper triangle linear system using a back substitution method. P_{U_k} is computed by $P_{U_k} = U_kU_k^\dagger$. Computing Z_k at Step 4 requires $U_kU_k^T$, one linear operator $\mathcal{A}$ and one adjoint $\mathcal{A}^*$. The linesearch procedure at Step 6 often requires i_k function evaluations as defined by (20) with one $U_kU_k^T$ and one linear operator $\mathcal{A}$.

The following corollary summarizes the convergence properties of Algorithm 3, which is a direct consequence of Lemma 2 and Theorem 1.

Corollary 1 *Let $\{U_k\}$ be the sequence generated by Algorithm 3. Then, under Assumption A.21, we have:*

(a) *There exists* $\underline{\alpha}_k := \min\left\{1, \frac{L\sigma_{\min}^3(U_k)}{2\|\nabla\Phi(U_k)\|_F}, \frac{3\sigma_{\min}(U_k)^4}{32\sigma_{\max}(U_k)^2\Phi'(U_k)}\right\} \in (0, 1]$ *such that*

$$\Phi(U_k + \alpha_kD_{U_k}) \le \Phi(U_k) - \frac{\alpha_k}{128L}\frac{\sigma_{\min}^2(U_k)}{\sigma_{\max}^4(U_k)}\|\nabla\Phi(U_k)\|_F^2, \quad \forall\alpha_k \in (0, \underline{\alpha}_k]. \tag{45}$$

Consequently, the linesearch procedure at Step 5 is well-defined (*i.e., it terminates after finite number of iterations* i_k).

(b) *If there exists* $\underline{\sigma} > 0$ *such that* $\sigma_{\min}(U_k) \ge \underline{\sigma}$ *for all* $k \ge 0$ *and* $\{U_k\}$ *is bounded, then one has* $\lim_{k\to\infty}\|\nabla\Phi(U_k)\|_F = 0$, *and any limit point of* $\{U_k\}$ *is stationary point of* (43).

The results in Corollary 1 is fundamentally different from [30], even when $\phi(\cdot) := (1/2)\|\cdot\|_2^2$ and $\mathcal{A}$ is identical, since we do not assume that B is positive definite in this case. When B is symmetric positive definite, we can apply the results in [30].

We note that Algorithm 2 can be specified to handle the symmetric case (43) by substituting Steps 4 and 5 by Steps 4 and 6 in Algorithm 3, respectively. We omit the details of this specification here.

6 Implementation remarks and extension

We discuss the implementation of Algorithms 1, 2 and 3 and provide an extension to nonsmooth cost ϕ.

6.1 Implementation remarks

We show how to generate appropriate initial points, to terminate the algorithms, and to update the penalty parameter ρ.

Computing initial points: Since (1) is nonconvex, the performance of the above algorithms strongly depends on an initial point. Principally, these algorithms still converge from any initial point. However, we propose to use the following simple procedure for finding an initial point: We first form a matrix $M \in \mathbb{R}^{m\times n}$ such that $\mathcal{A}(M) = B$. Then, we compute the r-truncated SVD of M as $[U_f, \Sigma_f, V_f]$ and form

$$U_0 := U_f(:, 1:r)\Sigma_f(1:r)^{1/2} \;\text{ and }\; V_0 := V_f(:, 1:r)\Sigma_f(1:r)^{1/2}.$$

In Algorithm 2, given $[U_0, V_0]$, we compute $W_0 := \mathcal{A}(U_0V_0^T) - B$ and set $\Lambda_0 := \mathbf{0}^l$.

Stopping criterions: We can implement different stopping criterions for Algorithms 1 and 2. The first criterion is based on the optimality condition (6) as

$$\max\left\{\|U_k^T\Phi'(U_kV_k^T)\|_F, \|\Phi'(U_kV_k^T)V_k\|_F\right\} \le \varepsilon_1 \max\left\{1, \|B\|_F\right\}, \tag{46}$$

where $\Phi'(UV^T) := \mathcal{A}^*\left(\nabla\phi(\mathcal{A}(UV^T) - B)\right)$. We can also terminate Algorithm 1 if

$$\max\left\{\|D_{U_k}\|_F, \|D_{V_k}\|_F\right\} \le \varepsilon_1 \max\left\{1, \|B\|_F\right\}. \tag{47}$$

We can add to Algorithm 2 the following condition for feasibility in (26):

$$\|U_kV_k^T - W_k\|_F \le \varepsilon_1 \max\left\{1, \|B\|_F\right\}. \tag{48}$$

When $\phi(\cdot) := (1/2)\|\cdot\|_F^2$ and the optimal value is zero, we also use

$$\|\mathcal{A}(U_kV_k^T) - B\|_F \le \varepsilon_2 \max\left\{1, \|B\|_F\right\}. \tag{49}$$

Similar stopping criterions are applied to Algorithm 3. These four stopping criterions are implemented in our codes and are used for numerical simulation in Section 7.

Penalty parameter update: Theoretically, we can fix any parameter ρ as indicated in (40). However, in Section 7, we follow the update rule used in [35] but with different parameters. We also use the full-step GN scheme at Step 4 in Algorithm 2.

6.2 Extension to nonsmooth objective function

We consider the nonsmooth objective function ϕ in (1). Then, the subproblem (28b) becomes

$$W_{k+1} := \operatorname*{argmin}_W\left\{\phi(W) + (\rho/2)\|W - Q_k\|_F^2\right\} = \operatorname{prox}_{\rho^{-1}\phi}(Q_k),$$

where $Q_k := \mathcal{A}(U_{k+1}V_{k+1}^T) - B + \rho^{-1}\Lambda_k$. In particular, if $\phi(\cdot) := \|\cdot\|_1$, then $\operatorname{prox}_{\rho^{-1}\phi(\cdot)}$ is the soft-thresholding operator, which can be computed in a closed form. Hence, we can modify Algorithm 2 to handle the nonsmooth objective function as done in [29]. Unfortunately, we do not have convergence guarantee for this algorithmic variant.

7 Numerical experiments

In this section, we verify the performance of three algorithms, Algorithms 1, 2 and 3. We first compare the full-step Gauss-Newton scheme and ADM. Next, we test this algorithm on a low-rank matrix approximation problem and compare it with standard SVDs. Finally, we apply Algorithms 1, 2 and 3 to solve 3 problems: matrix completion, matrix recovery with Pauli measurements in quantum tomography, and robust low-rank matrix recovery. Our code can be found online at `http://trandinhquoc.com/software.html`.

7.1 Comparison of Gauss-Newton and Alternating Direction Method

In order to observe the advantage of the GN scheme over the well-known ADM scheme for solving (1), we compare these algorithms on the following special case of (1):

$$\Phi^\star := \min_{U\in\mathbb{R}^{m\times r}, V\in\mathbb{R}^{n\times r}} \left\{ \Phi(U,V) := (1/2)\|\mathcal{A}(UV^T) - B\|_2^2 \right\}. \tag{50}$$

Since $\mathcal{A}$ is nonidentical, we upper bound $(1/2)\|\mathcal{A}(\cdot) - B\|_2^2$ by its quadratic surrogate

$$\begin{aligned}\tfrac{1}{2}\|\mathcal{A}(UV^T)-B\|_2^2 \le \tfrac{1}{2}\|\mathcal{A}(U_kV_k^T)-B\|_2^2 + \tfrac{1}{2}\|UV^T-(U_kV_k^T-L^{-1}\mathcal{A}^*(\mathcal{A}(U_kV_k^T)-B)))\|_2^2 \\ - \tfrac{1}{2L}\|\mathcal{A}^*(\mathcal{A}(U_kV_k^T) - B))\|_2^2,\end{aligned}$$

where $L := \|\mathcal{A}\|^2$ is the Lipschitz constant of the gradient of $(1/2)\|\mathcal{A}(\cdot) - B\|_2^2$.

Let $Z_k := L^{-1}\mathcal{A}^*(\mathcal{A}(U_kV_k^T) - B))$. Using this surrogate, we can write ADM as

$$\left\{\begin{array}{ll} U_{k+1} &:= \mathrm{argmin}_U \left\{ (1/2)\|UV_k^T - (U_kV_k^T - Z_k)\|_2^2 \right\}, \\ V_{k+1} &:= \mathrm{argmin}_V \left\{ (1/2)\|U_{k+1}V^T - (U_kV_k^T - Z_k)\|_2^2 \right\}. \end{array}\right. \tag{ADM}$$

We compare this algorithm and the following full-step GN scheme of (15):

$$(U_{k+1}, V_{k+1}) := \mathrm{argmin}_{U,V} \left\{ (1/2)\|U_kV^T + UV_k^T - (U_kV_k^T + Z_k)\|_2^2 \right\}. \tag{FsGN}$$

Clearly, ADM alternates between U and V and solves for them separately, while FsGN linearizes UV^T and solves for U_{k+1} and V_{k+1} simultaneously.

We implement these schemes in Matlab and running on a MacBook laptop with 2.6 GHz Intel Core i7, with 16GB memory. The input data is generated as follows. For $\mathcal{A}$, we generate an $(mn \times mn)$-matrix from either a fast Fourier transform (fft) or a standard Gaussian distribution, and take l random sub-samples from the rows of this matrix to form $\mathcal{A}$, where $l \le mn$. We generate $B = \mathcal{A}(U^\natural(V^\natural)^T) + \mathcal{N}(0, \sigma^2\mathbb{I})$, where $U^\natural \in \mathbb{R}^{m\times r}$ and $V^\natural \in \mathbb{R}^{n\times r}$ are given matrices, and $\mathcal{N}(0, \sigma^2\mathbb{I})$ is iid Gaussian noise of variance σ^2. We consider two cases: the underdetermined case with $l < r(m+n)$, and the overdetermined case with $l > r(m+n)$. In the first case, problem (50) always has solution with zero residual. We choose (U_0, V_0) randomly, which may not be in the local convergence region of the GN method.

Figure 1 shows the convergence behavior of the two algorithms. The right plot is $l = 2r(m+n)$, and the left one is $l = 0.5r(m+n)$, where $m = n = 512$ and $r = 32$.

We can see from Figure 1 that both algorithms perform very similarly in early iterations, but then FsGN gives better result in terms of accuracy (terminated around 10^{-9} in the overdetermined case due to the nonzero objective residual), while ADM is saturated at a certain level, and does not improve the objective values. In addition, Figures 1 and 2 show that the full-step Gauss-Newton scheme has a local linear convergence rate for the underdetermined case. However, as a compensation, FsGN requires one $(r \times m)$-matrix multiplication U^TU and one $(r \times r)$-inverse compared to ADM. This suggests that we can perform ADM in early iterations and switch to FsGN if ADM does not make significant progress to improve the objective values.

We test the underdetermined case by choosing a Gaussian operator $\mathcal{A}$ generated as $\mathcal{A} = \frac{1}{\sqrt{l}}\texttt{sprandn}(l, mn, 0.05)$. The convergence of two algorithms in this data is plotted

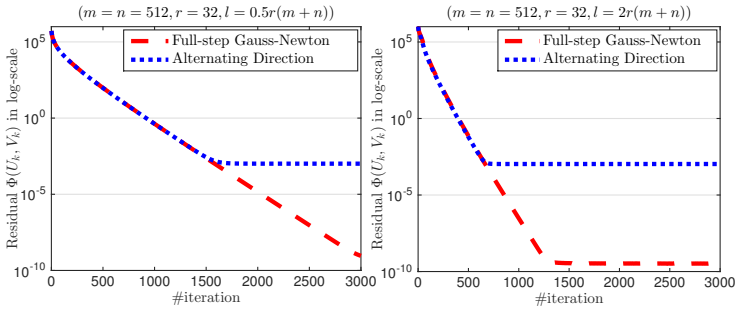

Fig. 1: A comparison between FsGN and ADM on 2 problem instances. Left: Underdetermined case —$l = 0.5r(m+n)$. Right: Overdetermined case—$l = 2r(m+n)$.

on the left side of Figure 2. Finally, we consider the effect of noise to both algorithms by adding a Gaussian noise with $\sigma^2 = 10^{-3}$. The performance of these algorithms is plotted on the right-hand side of Figure 2.

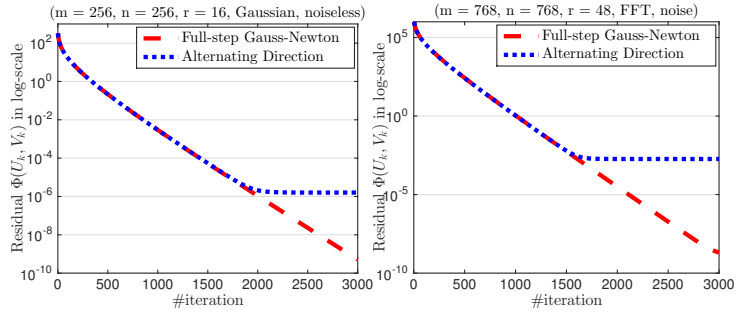

Fig. 2: A comparison between FsGN and ADM on 2 problem instances. Left: sparse Gaussian operator without noise. Right: subsampling FFT linear operator with noise

We can observe from Figure 2 the same behavior as in the previous test. Our FsGN still maintains a local linear convergence even with noise, while ADM is saturated at a certain level of the objective value.

7.2 Low-rank matrix factorization and linear subspace selection

We consider a special case of (1) by taking $\phi(\cdot) := (1/2)\|\cdot\|_F^2$ and $\mathcal{A} = \mathbb{I}$ as

$$\Phi^\star := \min_{U,V} \left\{ \Phi(U,V) := (1/2)\|UV^T - B\|_F^2 : U \in \mathbb{R}^{m\times r}, V \in \mathbb{R}^{n\times r} \right\}. \tag{51}$$

Although this problem has a closed form solution by truncated SVD, our objective is to compare the full-step GN variant of Algorithm 1 with standard Matlab singular value routines: `svds` and `lansvd`. The full-step GN scheme for (51) is presented as

$$V_{k+1}^T := U_k^\dagger B \quad \text{and} \quad U_{k+1} := U_k + (B - U_k^T V_{k+1})(V_k^\dagger)^T. \tag{52}$$

At each iteration, (52) requires two $(r\times r)$-matrix inverses $U_k^T U_k$ and $V_k^T V_k$, and three $(m \times r)$- or $(n \times r)$- matrix - $(r \times r)$-matrix multiplications. We compute these two inverses by Cholesky. We note that we do not form the $(m \times n)$-matrix $U_k V_k^T$ at each iteration, but we can occasionally compute it to check the objective value if required.

We choose $U_0 := [\mathbb{I}_r, \mathbf{0}^T_{(m-r)\times r}]^T$ and $V_0 := [\mathbf{0}^T_{(n-r)\times r}, \mathbb{I}_r]^T$ as a starting point, where $\mathbb{I}_r$ is the identity matrix.

The scheme (52) generates two low-rank matrices U_k and V_k so that $U_k V_k^T \approx B$. To orthonormalize U_k and V_k, we can perform a Rayleigh–Ritz (RR) procedure:

- Compute $[Q_u, R_u] = \texttt{qr}(U_k, 0)$ and $[Q_v, R_v] = \texttt{qr}(V_k, 0)$, the two economic QR-factorizations of size r.
- Compute $[U_r, \Sigma_r, V_r] = \texttt{svd}(Q_u^T B Q_v)$ the singular value decomposition of the $r \times r$ matrix $Q_u^T B Q_v$.
- Then form $U = Q_u U_r$ and $V = Q_v V_r$ to obtain two orthogonal matrices U and V of the size $m \times r$ and $n \times r$, respectively so that $[U, \Sigma, V] = \texttt{svds}(B, r)$.

Note that (52) is different from [30] working on a symmetric positive definite matrix.

Now, we test (52) combining with the Rayleigh–Ritz procedure, and compare it with `svds` and `lansvd`. We generate an input matrix B of size $m \times n$ with rank r as follows. Once m is chosen, we set $n = m$ and either $r = 0.01 \times m$ or $r = 0.05 \times m$ (which is either 1% of problem size or 5% of problem size, respectively). Then, we generate matrix $B \in \mathbb{R}^{m\times n}$ using the following Matlab code:

```
min_mn      = min(m, n);
nnz_sig_vec = [1:1:r].^(-0.01);
sig_vec     = [nnz_sig_vec(:); zeros(min_mn-r, 1)];
n_sig_vec   = sqrt(length(sig_vec))/norm(sig_vec(:), 2)*sig_vec;
B           = gallery('randcolu', n_sig_vec, max(m, n), 1);
G           = sprandn(m, n, nnz(B)/(m*n));
M_mat       = B + 0.1*norm(B, 'fro')*G/norm(G, 'fro');
```

If B is generated as above, then its singular values σ_i is clustered into parts: $\sigma_i = i^{-0.01}$ for $i = 1, \cdots, r$, and $\sigma_i = 0$ for $i = r+1, \cdots, \min\{m, n\}$. In addition, an idd Gaussian noise $\frac{\|B\|_F}{10\|G\|_F} G$ is added to B, where $G = \mathcal{N}(0, \sigma\mathbb{I})$, with σ being the sparsity of B. We terminates (52) using either (46) or (47) with $\varepsilon_1 = 10^{-6}$ or $\varepsilon_2 = 10^{-4}$, respectively. We also terminate `svds` and `lansvd` using $\texttt{tol} = 10^{-4}$.

The performance of three algorithms in terms of computational time vs. problem size is plotted in Figure 3 for 10 problems from $m = n = 1,000$ to $m = n = 10,000$, carried out on a MacBook laptop with 2.6 GHz Intel Core i7, with 16GB memory. We run each problem size 10 times and compute the averaging computational time. The abbreviation `Full-step Gauss-Newton` indicates the time of both scheme (52) and Rayleigh-Ritz procedure, while `Full-step Gauss-Newton without RR` only counts for the time of (52). The left of Figure 3 shows the performance with $r = 0.01 \times m$, while the right of Figure 3 reveals the case $r = 0.05 \times m$.

Clearly, when the rank r is about 1% of problem size, (52) is comparable to `lansvd` while it is slightly better than `svds`. However, when the rank r is increased to 5% of problem size, (52) clearly outperforms both `lansvd` and `svds`.

7.3 Recovery with Pauli measurements in quantum tomography

We consider a d spin-1/2 systems with unknown state S as described in [21]. A d-qubit Pauli matrix is given by the form $w = \otimes_{i=1}^d w_i$, where $w_i \in \{\mathbf{1}, \sigma^x, \sigma^y, \sigma^z\}$ a given set of elements. There are n^2, $n = 2^d$, such a matrices denoted by $w(s)$ with $s \in \{1, \cdots, n^2\}$. A compressive sensing procedure takes m integer numbers $s_1, \cdots, s_m \in$

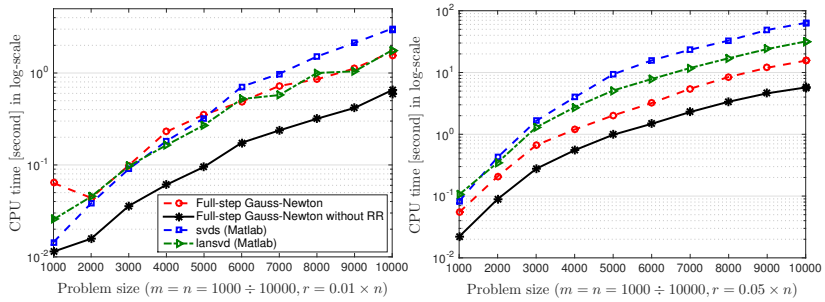

Fig. 3: A comparison between the full-step Gauss-Newton method, `Matlab SVDS`, and `Matlab LanSVD` on 10 problem sizes (from $1,000$ to $10,000$), and two different ranks. The result is on average of 10 random runs for each problem size.

$\{1, \cdots, n^2\}$ randomly and measures the expected values trace $(Sw(s_i))$. Then, it solves the following convex problem to construct the unknown states:

$$\text{trace}\,(X) = 1, \quad \text{trace}\,(Xw(s_i)) = \text{trace}\,(w_i S) \;\; (i = 1, \cdots, m). \tag{53}$$

As shown in [21], the number of measurement m to reconstruct the quantum states can be estimated as $m = cnr \log^2 n \ll n^2$ for some constant c and the rank r.

Given that X characterizes a density matrix, which is positive semidefinite Hermitian, we instead consider the following least-squares formulation of (53):

$$\min_{X \in \mathcal{H}_+^n} \left\{ (1/2)\|B - \mathcal{A}(X)\|_F^2 : \text{trace}(X) = 1 \right\}, \tag{54}$$

where $\mathcal{H}_+^n$ is the set of positive semidefinite Hermitian matrices of size n, and $\mathcal{A}$ and B are the measurement operator and observed measurements obtained from (53). Assume that $X = UU^T$, where $U \in \mathbb{C}^{n\times 1}$, we can write this problem into

$$\min_{U \in \mathbb{C}^{n\times 1}} \left\{ (1/2)\|B - \mathcal{A}(UU^T)\|_F^2 \right\}, \tag{55}$$

where $\mathbb{C}^{n\times 1}$ is the set of $(n \times 1)$ - complex matrices. Clearly, problem (55) falls into the special form (43) of (1) which can be solved by Algorithm 3.

We test Algorithm 3 and compared it with the Frank-Wolfe methods proposed in [23]. We use both standard Frank-Wolfe and its line-search variant. We generate an initial point $U_0 := [\mathbb{I}_r, \mathbf{0}^T_{(n-r)\times r}]^T$ and terminate Algorithm 3 using either (46), (47) or (49) with $\varepsilon_1 = 10^{-9}$ and $\varepsilon_2 = 10^{-6}$, respectively. We generate $\mathcal{A}$ and B using procedures in [21]. We perform two cases: noise and noiseless. In the noisy case, we set S to be $0.99S + 0.01\mathbb{I}_n/n$ before computing the observed measurement B. In this example, Frank-Wolfe's algorithms take long time to reach a high accuracy, we terminate them if $\|\mathcal{A}(X) - B\|_F \le 10^{-3}\sqrt{2}\,\|B\|_F$, which is different from Algorithm 3.

We test on 4 problems of the size d with $d \in \{10, 11, 12, 13\}$ being the number of qubits running one a single node of an Intel(R) Xeon(R) 2.67GHz processor with 4GB memory, but can share up to 320GB RAM. The results and performance of three algorithms are reported in Table 1, where m is the number of measurements, $n = 2^d$, iter is the number of iterations, time[s] is the computational time in seconds.

Table 1: Numerical results of three algorithms on noiseless and noisy data for the quantum tomography experiment.

			Algorithm 3			Frank-Wolfe without LS			Frank-Wolfe with LS		
#qubits	m	n	iter	time[s]	$\frac{\|B-\mathcal{A}(X)\|_F}{\|B\|_F}$	iter	time[s]	$\frac{\|B-\mathcal{A}(X)\|_F}{\|B\|_F}$	iter	time[s]	$\frac{\|B-\mathcal{A}(X)\|_F}{\|B\|_F}$
The noiseless case											
10	14196	1024	26	12.25	3.21e-06	1707	664.90	1.65e-03	322	129.35	1.62e-03
11	31231	2048	25	71.60	2.64e-06	1654	2803.18	1.61e-03	370	593.56	1.54e-03
12	68140	4096	25	696.27	1.78e-06	1577	17990.98	1.56e-03	254	1741.19	1.54e-03
13	147635	8192	27	1516.97	1.73e-06	648	20574.13	3.68e-03	303	9654.69	1.52e-03
The depolarizing noisy case (1%)											
10	14196	1024	24	16.07	8.99e-06	1711	692.16	1.66e-03	238	78.22	1.66e-03
11	31231	2048	23	94.98	8.80e-06	1663	2683.90	1.62e-03	258	423.27	1.61e-03
12	68140	4096	23	589.73	6.03e-06	1585	12146.01	1.56e-03	247	1892.66	1.56e-03
13	147635	8192	24	3684.57	8.76e-06	648	20537.15	3.70e-03	292	8691.90	1.53e-03

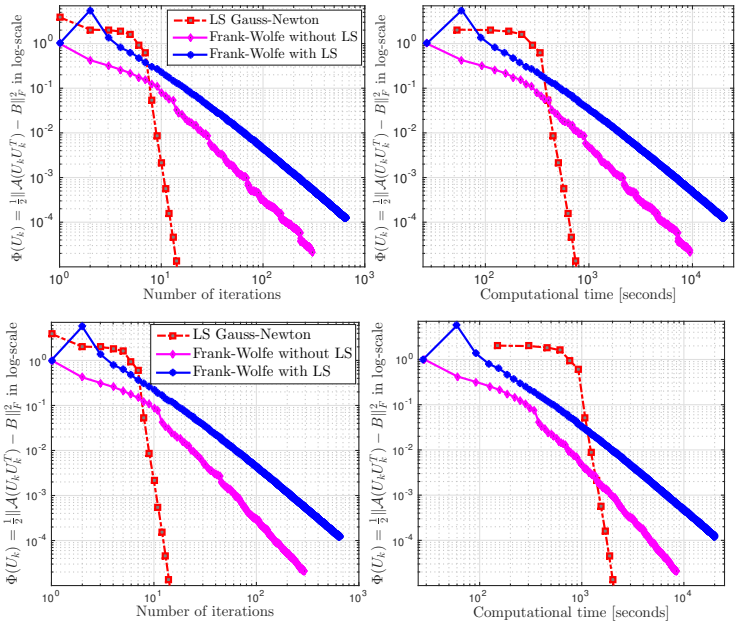

Fig. 4: A comparison of three algorithms for noiseless case (first row) and for the 0.01 depolarizing noisy case (second row).

Convergence behavior of three algorithms for both noiseless and noisy cases with $d = 13$ is also plotted in Figure 4.

We can observe from our results that Algorithm 3 highly outperforms two Frank-Wolfe's algorithms. It also reaches a highly accurate solution after few iterations. However, each iteration of Algorithm 3 is more expensive than of Frank-Wolfe's algorithms. As seen from Figure 4, Algorithm 3 behaves like super-linearly convergent.

7.4 Matrix completion

Our next experiment is the well-known matrix completion in recommender systems [10, 16, 40]. This problem is a special case of (1):

$$\min_{U,V}\left\{\|(1/2)\mathcal{P}_\Omega(UV^T) - B\|_F^2 : U \in \mathbb{R}^{r\times m}, V \in \mathbb{R}^{r\times n}\right\}, \tag{56}$$

where $\mathcal{P}_\Omega$ is a selection operator on an index set Ω, and B are observed entries.

There are two major approaches to solve (56). The first one is using a convex relaxation for the rank constraint via nuclear or max norm. Methods based on this approach have been widely developed in the literature, including SVT [7], and [accelerated] gradient descent [16,37]. The second approach is using nonconvex optimization, including, e.g., OpenSpace [25] and LMaFit [29,40].

In this experiment, we select the most efficient algorithms for our comparison: the over-relaxation alternating direction method (LMaFit) in [40], and the accelerated proximal gradient method (APGL) in [37]. We will test four algorithms on synthetic and three first algorithms on real datasets.

Synthetic data: Since data in rating systems is often integer, our synthetic data set is generated as follows. We first randomly generate two integer matrices U and V whose entries are in $\{1, \cdots, 5\}$ of the size $m \times r$ and $n \times r$, respectively. Then, we form $M = UV^T$. Finally, we randomly take either 50% or 30% entries of M as output matrix B. We can also add a standard Gaussian noise to B if necessary. A Matlab script for generating such a dataset is given below.

```
U_org    = randi(5, m, r);
V_org    = randi(5, n, r);
M_org    = U_org*V_org';
s        = round(0.5*m*n);
Omega    = randsample(m*n, s);
M_omega  = M_org(Omega);
B        = M_omega + sigma*randn(size(M_omega));
```

We first test these algorithms with a fixed rank r and 50% randomly observed entries, which is relative dense. We terminate Algorithms 1 and 2 using the conditions given in Subsection 6.1 with $\varepsilon_1 = 10^{-6}$ and $\varepsilon_2 = 10^{-4}$, respectively. We also terminate LMaFit and APGL with the same tolerance $\texttt{tol} = 10^{-4}$. The initial point is computed by a truncated SVD as in Subsection 6.1 for three first algorithms.

The test is carried out on 10 problems of different sizes running on a single node of an Intel(R) Xeon(R) 2.67GHz processor with 4GB memory, but can share up to 100GB RAM. We run each problem size 10 times and compute the average result and performance. The problem sizes and results are reported in Table 2 for different two ranks. The rank r is chosen as $r = 0.01 \times m$, and $r = 0.05 \times m$, which correspond to 1%, and 5% of problem size. Here, iter and time[s] are the iteration number of iterations and computational time in seconds, respectively; rank is the rank of $U_k V_k^T$ given by the algorithms; and

$$\delta f_k := \|\mathcal{P}_\Omega(U_k V_k^T) - B\|_F / \|B\|_F, \quad \text{and} \quad \text{NMAE} := C^{-1} \sum_{(i,j)\in\Omega} \left|(U_k V_k^T)_{ij} - B_{ij}\right|,$$

are the relative objective residual; and the Normalized Mean Absolute Error, respectively, where $C := (\max_{i,j} B_{ij} - \min_{ij} B_{ij})|\Omega|$.

The results in Table 2 show that both Algorithms 1 and 2 produce similar results as LMaFit in terms of the relative objective residual and NMAE. When the rank is small (i.e., 1% of problem size), Algorithm 1 and LMaFit have similar number of iterations, but LMaFit has better computational time. When the rank is increasing up to 5% of problem size, both Algorithm 1 and Algorithm 2 require fewer iterations than LMaFit,

Table 2: Comparison of four algorithms on synthetic integer datasets without noise

			Algorithm 1					Algorithm 2				
m	n	r	iter	time[s]	δf_k	NMAE	rank	iter	time[s]	δf_k	NMAE	rank
1000	2000	10	15.9	2.11	4.15e-05	1.39e-05	10	30.0	2.07	8.34e-05	3.55e-05	10
1000	2000	50	20.8	4.34	6.91e-05	5.78e-05	50	37.6	4.43	9.61e-05	7.83e-05	50
2500	2500	25	14.3	8.05	5.31e-05	2.97e-05	25	31.1	9.18	1.04e-04	6.18e-05	25
2500	2500	125	26.3	28.94	7.35e-05	8.18e-05	125	35.2	23.68	1.05e-04	1.32e-04	125
5000	5000	50	15.7	53.40	5.42e-05	3.90e-05	50	32.0	56.71	9.87e-05	7.80e-05	50
5000	5000	250	23.6	180.70	7.94e-05	1.35e-04	250	35.0	165.89	1.10e-04	1.94e-04	250
5000	7500	50	14.9	76.93	5.10e-05	3.64e-05	50	32.0	85.72	8.51e-05	6.65e-05	50
5000	7500	250	23.7	273.30	7.61e-05	1.22e-04	250	35.0	245.93	9.97e-05	1.68e-04	250
10000	10000	100	16.2	289.14	5.99e-05	5.86e-05	100	32.2	319.92	1.10e-04	1.16e-04	100
10000	10000	500	24.8	1303.01	8.02e-05	1.75e-04	500	35.0	1173.38	1.14e-04	2.60e-04	500
			LMaFit [40]					APGL [37]				
m	n	r	iter	time[s]	δf_k	NMAE	rank	iter	time[s]	δf_k	NMAE	rank
1000	2000	10	13.3	0.94	4.74e-05	1.43e-05	10	28.0	4.29	3.31e-04	1.40e-04	10
1000	2000	50	109.8	12.13	2.71e-04	1.51e-04	50	28.6	6.79	1.06e-02	9.02e-03	41.6
2500	2500	25	10.0	3.10	6.98e-05	3.86e-05	25	29.0	16.64	5.06e-04	3.07e-04	25
2500	2500	125	135.3	85.78	2.99e-04	2.59e-04	125	31.6	20.00	1.92e-02	2.43e-02	5
5000	5000	50	10.0	18.43	5.57e-05	4.30e-05	50	30.6	81.69	8.48e-04	6.73e-04	50.2
5000	5000	250	140.9	631.58	6.70e-05	8.58e-05	250	30.4	60.75	1.38e-02	2.44e-02	5
5000	7500	50	10.1	28.21	4.38e-05	2.92e-05	50	30.8	122.47	7.35e-04	5.76e-04	50
5000	7500	250	126.8	845.90	7.02e-05	7.30e-05	250	30.5	90.74	1.38e-02	2.33e-02	5
10000	10000	100	11.0	112.82	3.10e-05	3.24e-05	100	32.7	266.16	2.15e-02	2.28e-02	5
10000	10000	500	120.4	3818.05	6.25e-05	8.63e-05	500	30.3	206.86	9.85e-03	2.26e-02	5

and outperform this solver in terms of computational time. In this experiment, the number of iterations in Algorithm 2 is very similar for all the test cases, from 30 to 38 iterations, and similar to APGL. We note that we fix the rank in the first three algorithms, since APGL uses a convex approach, it cannot predict well an approximate rank if it is 5% of problem size, or when problem size is increasing.

Now, we add idd Gaussian noise $\mathcal{N}(0, \sigma\mathbb{I})$ with $\sigma = 0.01$ to B as $B := B^\natural + 5 \times \mathcal{N}(0, \sigma\mathbb{I})$, and only randomly take 30% observed entries. The convergence behavior of three algorithms for one problem instance with $m = n = 5000$ is plotted in Figure 5. When the rank $r = 0.01m$ (i.e., 1% problem size), LMaFit outperforms Algorithms 1

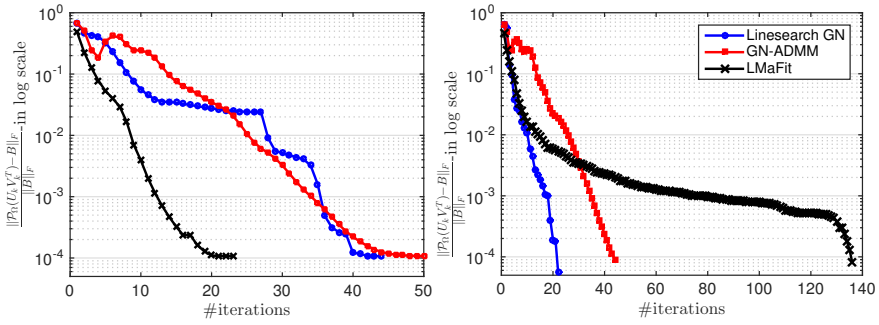

Fig. 5: The convergence behavior of three algorithms for the case $m = n = 5000$ with noise ($\sigma = 0.01$) and 30% observed entries (Left: $r = 0.01m$, Right: $r = 0.025m$).

and 2 in terms of iterations, but when the rank $r = 0.025m$ (i.e., 2.5% problem size), Algorithms 1 and 2 are much better than LMaFit. Algorithm 1 works really well in the second case, and takes only 22 iterations. We also observe the monotone decrease in Algorithm 1 as guaranteed by our theory, but not in Algorithm 2.

Table 3: Comparison of four algorithms on synthetic integer MC datasets with noise.

			Algorithm 1					Algorithm 2				
m	n	r	iter	time[s]	δf_k	NMAE	rank	iter	time[s]	δf_k	NMAE	rank
1000	2000	10	40.8	3.56	5.33e-04	2.27e-04	10	40.5	2.24	5.32e-04	2.26e-04	10
1000	2000	25	49.1	5.50	6.05e-04	2.76e-04	25	62.0	4.62	2.09e-04	1.31e-04	25
5000	5000	50	19.5	39.82	1.10e-04	8.71e-05	50	45.0	67.70	1.09e-04	8.63e-05	50
5000	5000	125	16.6	56.70	7.90e-05	9.58e-05	125	40.0	103.45	9.50e-05	1.19e-04	125
			LMaFit [40]					APGL [37]				
m	m	r	iter	time[s]	δf_k	NMAE	rank	iter	time[s]	δf_k	NMAE	rank
1000	2000	10	31.6	1.71	5.31e-04	2.26e-04	10	28.0	3.08	6.34e-04	2.70e-04	10
1000	2000	25	121.0	8.55	2.08e-04	1.31e-04	25	30.7	5.86	9.87e-04	5.93e-04	25
5000	5000	50	20.0	30.39	1.07e-04	8.49e-05	50	28.5	52.96	4.97e-03	3.82e-03	48.2
5000	5000	125	48.0	121.11	7.19e-05	7.34e-05	125	31.3	46.99	1.92e-02	2.42e-02	5

Finally, we test three first algorithms on 2 problems with 30% observed entries in B and with iid Gaussian noise $\mathcal{N}(0, 0.01\mathbb{I})$). The results of this test is reported in Table 3. LMaFit remains working well for low-rank cases, while getting slower when the rank r increases. Algorithms 1 and 2 have similar performance in this case.

"Real" data: Now, we test three algorithms: Algorithm 1, Algorithm 2 and LMaFit on "real" MovieLens and Jester jokes datasets available on `http://grouplens.org/datasets/movielens/`. For the MovieLens dataset, we test our algorithms on 5 problems: "movie-lens-latest (small)", "movie-lens" 100k, 1M, 10M and 20M, which we abbreviate by "movie(s)", and "moviexM" in Table 4, respectively. We also test all problems in Jester joke dataset: "jester-1", "jester-2", "jester-3" and "jester-all".

In this test, since the data in "movie10M" and "movie20M" is sparse, we run three algorithms on a MacBook laptop with 2.6 GHz Intel Core i7, with 16GB memory. We use mex-routines to compute $\mathcal{P}_\Omega(UV^T)$ in three algorithms to avoid forming U^TV. We terminates our algorithms based on the objective value obtained from LMaFit such that three algorithms have similar objective value.

The result is summarized in Table 4, where we add a new measurement $\delta x_k := \frac{1}{|\Omega|}\sum_{(i,j)\in\Omega}\left|\lfloor(U_kV_k^T)_{ij}\rfloor - B_{ij}\right|$ to measure the agreement ratio between recovered matrix $M_k := U_kV_k^T$ and the observed data B projected onto Ω. Due to our stopping criterion, three algorithms provide similar results in terms of the objective residual, solution aggrement and NMAE. LMaFit works well on the Jester jokes dataset, but the computational time on these problems is relatively small. Algorithm 2 works well on Movielen dataset, especially for Movie 10MB and Movie 20MB. As mentioned previously, Algorithm 1 often achieve better solution in terms of accuracy if we run it long enough, while LMaFit and Algorithm 2 can be used to achieve a low or medium accurate solution for matrix completion.

Table 4: Summary of results of four algorithms for MC on "real" datasets.

			Algorithm 1			Algorithm 2			LMaFit [40]		
Name	m	n	iter	time[s]	δf_k	iter	time[s]	δf_k	iter	time[s]	δf_k
jester-1	24983	100	45	11.60	1.75e-01	59	11.35	1.75e-01	36	4.78	1.75e-01
jester-2	23500	100	41	9.93	1.77e-01	57	11.07	1.77e-01	34	5.51	1.77e-01
jester-3	24938	100	30	5.15	9.04e-04	32	4.94	9.66e-04	25	2.13	9.26e-04
jester-all	73421	100	48	35.12	1.65e-01	57	30.12	1.65e-01	36	12.21	1.65e-01
movie(s)	668	10325	200	16.69	1.64e-03	87	7.14	1.58e-03	200	44.18	1.58e-03
movie100k	943	1682	200	9.66	1.03e-02	84	4.87	1.00e-02	200	15.63	1.00e-02
movie1M	6040	3706	79	41.71	1.18e-01	42	21.96	1.19e-01	70	49.84	1.18e-01
movie10M	69878	10677	69	109.02	2.14e-01	33	38.32	2.15e-01	61	40.48	2.14e-01
movie20M	138493	26744	89	307.22	2.30e-01	37	117.23	2.30e-01	87	133.86	2.30e-01

			Algorithm 1			Algorithm 2			LMaFit [40]		
Name	m	n	rank	δx_k	NMAE	rank	δx_k	NMAE	rank	δx_k	NMAE
jester-1	24983	100	80	4.71e-01	2.29e-02	80	4.71e-01	2.36e-02	80	4.59e-01	2.30e-02
jester-2	23500	100	80	4.82e-01	2.35e-02	80	4.82e-01	2.42e-02	80	4.78e-01	2.39e-02
jester-3	24938	100	80	8.78e-04	1.08e-05	80	8.78e-04	7.22e-05	80	9.87e-04	2.08e-05
jester-all	73421	100	80	4.09e-01	1.95e-02	80	4.09e+01	2.05e-02	80	3.95e-01	1.98e-02
movie(s)	668	10325	100	1.36e-01	3.76e-04	100	1.36e-01	6.91e-04	100	1.36e-01	3.97e-04
movie100k	943	1682	100	1.10e-04	5.24e-03	100	1.10e-04	4.87e-03	100	1.00e-04	4.64e-03
movie1M	6040	3706	100	2.34e-01	8.28e-02	100	2.34e-01	8.44e-02	100	2.32e-01	8.32e-02
movie10M	69878	10677	20	5.86e-01	1.34e-01	20	5.86e-01	1.35e-01	20	5.81e-01	1.34e-01
movie20M	138493	26744	10	6.29e-01	1.42e-01	10	6.29e-01	1.42e-01	10	6.30e-01	1.42e-01

7.5 Robust low-rank matrix recovery

We consider the nonsmooth problem

$$\min_{U,V}\left\{\|UV^T - B\|_1 : U \in \mathbb{R}^{m\times r}, V \in \mathbb{R}^{n\times r}\right\}, \tag{57}$$

where $\|Z\|_1 := \sum_{ij}\left|Z_{ij}\right|$ is the ℓ_1-norm of Z. This a low-rank matrix recovery problem with the ℓ_1-norm, which can be referred to as a robust recovery as opposed to the standard square loss. This formulation is often used in background extraction [35].

Clearly, we can solve (57) using our GN-ADMM scheme in Subsection 6.2, which can be simply described as follows:

$$\begin{cases} V_{k+1}^T &:= U_k^{\dagger}(B + W_k - \Lambda_k),\\ U_{k+1} &:= U_k + \left(B + W_k - \Lambda_k - U_kV_{k+1}^T\right)(V_k^{\dagger})^T,\\ W_{k+1} &:= \mathrm{prox}_{\rho^{-1}\|\cdot\|_1}\left(U_{k+1}V_{k+1}^T + \Lambda_k - B\right)\\ \Lambda_{k+1} &:= \Lambda_k + (U_{k+1}V_{k+1}^T - W_{k+1}). \end{cases} \tag{58}$$

We apply this scheme to solve the (57) using video surveillance dataset at `http://perception.i2r.a-star.edu.sg/bk_model/bk_index.html`. We implement the scheme (58) in Algorithm 2 and compare it with the augmented Lagrangian method proposed in [35], which we denote by L1-LMaFit. We use the same strategy as in L1-LMaFit to update the penalty parameter ρ, while using $U_0 := [\mathbb{I}_r, \mathbf{0}_{(m-r)\times r}]$ and $V_0 := [\mathbb{I}_r, \mathbf{0}_{(n-r)\times r}]$ as an initial point. As suggested in [35], we choose the rank r to be $r = 1$ when testing gray-scale video data. As experienced, L1-LMaFit was based on alternating direction idea, which can be saturated. Hence, we run both algorithm up to 100 iterations to observe. The computational time and the relative objective value $\|U_kV_k^T - B\|_1/\|B\|_1$ of these two algorithms are reported in Table 5.

Table 5: Summary of results of two algorithms for video background extraction.

Video data			Algorithm 2		L1-LMaFit [35]	
Video	Resolution	#Frames	Time	$\|U_kV_k^T - B\|_1/\|B\|_1$	Time	$\|U_kV_k^T - B\|_1/\|B\|_1$
Escalator	130×160	200	12.48	9.434063×10^{-2}	13.30	9.435117×10^{-2}
Fountain	128×160	200	13.27	4.197912×10^{-2}	13.71	4.198963×10^{-2}
Bootstrap	120×160	250	15.76	13.103802×10^{-2}	16.91	13.107209×10^{-2}
Curtain	128×160	250	18.43	2.965992×10^{-2}	25.45	2.969248×10^{-2}
Campus	128×160	300	24.83	9.315523×10^{-2}	30.10	9.316343×10^{-2}
Hall	144×176	300	31.63	5.708911×10^{-2}	39.05	5.709121×10^{-2}
ShoppingMall	256×320	350	82.22	4.442732×10^{-2}	85.48	4.442907×10^{-2}
WaterSurface	128×160	350	35.92	3.607625×10^{-2}	40.25	3.607747×10^{-2}

We can observe from Table 5 that the computational time in both algorithms is almost the same. This is consistent with our theoretical result, since the complexity-per-iteration of two algorithms is almost the same when we choose $r = 1$. However, Algorithm 2 provides a slightly better objective value since it still improves the objective when running further as compared to L1-LMaFit. Here, we use the full-step variant of Algorithm 2, a fast convergence guarantee can be achieved when a good initial point is provided. This remains unclear in L1-LMaFit [35]. Unfortunately, global convergence of our variant as well as L1-LMaFit has not been known yet.

8 Conclusion

We have proposed a Gauss-Newton framework for low-rank matrix nonconvex optimization. Our method features several advantages from classical Gauss-Newton (GN) method such as fast local convergence, achieving high accuracy solutions compared to the well-known alternating direction (AD) method. We proposed a line-search GN algorithm and show both global and local convergence under standard assumptions. We have also specified this algorithm to the symmetric case, where AD is not applicable. Then, we have combined our GN framework with the alternating direction method of multipliers (ADMM) to design a new GN-ADMM that has global convergence guarantee and low-complexity-per-iteration. Several numerical experiments have been presented to demonstrate the theory and show the advantages of nonconvex optimization approaches. The theory presented in this paper can be extended to different directions, including constrained low-rank matrix optimization, and low-rank tensor optimization. In addition, several important applications such as robust principal component analysis, phase-retrieval, computer vision, covariance analysis, and graph cluster are interesting to treat by applying our methods.

Acknowledgments We would like to thank A. Yurtsever (LIONS, EPFL) for providing us the Matlab code of Frank-Wolfe's algorithms using in Subsection 7.3.

A The proof of technical results

We provide the full proofs of all technical results in the main text.

A.1 The proof of Lemma 1: Closed form of Gauss-Newton direction

Le us define $x := [\mathrm{vec}\left(D_V^T\right), \mathrm{vec}\left(D_U\right)]$ and $b := [\mathrm{vec}(U^TB), \mathrm{vec}(BV)]$. Then, we can write (12) as $\mathcal{B}x = b$, where $\mathcal{B} := \begin{bmatrix} \mathbb{I}_n \otimes U^TU & V \otimes U^T \\ V^T \otimes U & V^TV \otimes \mathbb{I}_m \end{bmatrix}$. We can show that

$$\mathcal{B} = \begin{bmatrix} (\mathbb{I}_n \otimes U^T)(\mathbb{I}_n \otimes U) & (\mathbb{I}_n \otimes U^T)(V \otimes \mathbb{I}_m) \\ (V^T \otimes \mathbb{I}_m)(\mathbb{I}_n \otimes U) & (V^T \otimes \mathbb{I}_m)(V \otimes \mathbb{I}_m) \end{bmatrix} = \begin{bmatrix} \mathbb{I}_n \otimes U^T \\ V^T \otimes \mathbb{I}_m \end{bmatrix} \begin{bmatrix} \mathbb{I}_n \otimes U & V \otimes \mathbb{I}_m \end{bmatrix}.$$

By [1, Fact. 7.4.24], we have rank $([\mathbb{I}_n \otimes U, V \otimes \mathbb{I}_m]) \leq (m+n-r)r$. Hence, rank $(\mathcal{B})$ in (12) does not exceed $r(m+n-r) < r(m+n)$.

Next, we can rewrite $b = [(\mathbb{I}_n \otimes U^T)\mathrm{vec}(B); (V^T \otimes \mathbb{I}_m)\mathrm{vec}(B)]$. If we consider the extended matrix $\bar{\mathcal{B}} := [\mathcal{B}, b]$, then we can express it as

$$\bar{\mathcal{B}} = \begin{bmatrix} \mathbb{I}_n \otimes U^T \\ V^T \otimes \mathbb{I}_m \end{bmatrix} \begin{bmatrix} \mathbb{I}_n \otimes U & V \otimes \mathbb{I}_m & \mathrm{vec}(B) \end{bmatrix}.$$

This shows that rank $\left(\bar{\mathcal{B}}\right) =$ rank $(\mathcal{B})$. Hence, (12) has solution.

Now, we find the closed form (14). Since rank $(U) =$ rank $(V) = r$, both U^TU and V^TV are invertible. Pre-multiplying the first equation of (12) by $(U^TU)^{-1}$ and rearranging the result, we have

$$D_V^T = (U^TU)^{-1}U^T(Z - D_UV^T). \tag{59}$$

Substituting this into the second equation of (12) we get

$$(\mathbb{I} - U(U^TU)^{-1}U^T)D_VV^TV = (\mathbb{I} - U(U^TU)^{-1}U^T)ZV. \tag{60}$$

Using the definition of the projections P_U, P_V, $P_U^\perp$ and $P_V^\perp$, we have from (60) that $P_U^\perp D_V V^T V = P_U^\perp ZV$. Post-multiplying this expression by $(V^TV)^{-1}$, we obtain

$$P_U^\perp D_V = P_U^\perp ZV(V^TV)^{-1}. \tag{61}$$

Assume that $D_U := D_U^0 + U\hat{D}_r$, where D_U^0 is a given vector in the null space of U^T, i.e., $U^TD_U^0 = 0$, and $\hat{D}_r \in \mathbb{R}^{r\times r}$ is an arbitrary matrix. Substituting this expression into (61) and noting that $P_U^\perp U = 0$, we obtain

$$D_U^0 = D_U^0 - U(U^TU)^{-1}U^TD_U^0 + P_U^\perp U\hat{D}_r = P_U^\perp ZV(V^TV)^{-1}.$$

Hence, we finally get

$$D_U = P_U^\perp ZV(V^TV)^{-1} + U\hat{D}_r, \quad \text{for any } \hat{D}_r \in \mathbb{R}^{r\times r}, \tag{62}$$

which is exactly the first term in (13). Substituting this D_U into (59) to yield the second term of (13) as

$$\begin{aligned} D_V^T &= (U^TU)^{-1}U^T\left(Z - P_U^\perp ZV(V^TV)^{-1}V^T - U\hat{D}_rV^T\right) \\ &= (U^TU)^{-1}U^TZ - U^TU)^{-1}U^TP_U^\perp ZV(V^TV)^{-1}V^T - \hat{D}_rV^T \\ &= (U^TU)^{-1}U^TZ - \hat{D}_rV^T. \end{aligned}$$

Since $\hat{D}_r$ is arbitrary in $\mathbb{R}^{r\times r}$, we choose $\hat{D}_r := \frac{1}{2}(U^TU)^{-1}U^TZV(V^TV)^{-1} \in \mathbb{R}^{r\times r}$. Substituting this choice into (13), we obtain

$$D_U = \big(\mathbb{I}_m - (1/2)P_U\big)ZV(V^TV)^{-1} \quad \text{and} \quad D_V^T = (U^TU)^{-1}U^TZ\big(\mathbb{I}_n - (1/2)P_V\big),$$

which is (14). Hence, the solution set of (12) forms an $(r\times r)$-linear subspace.

Finally, let us denote the residual term in the objective of (11) by $R(D_U, D_V) := UD_V^T + D_UV^T - Z$. Then, using the expression (13) we can easily show that

$$\begin{aligned} R(D_U, D_V) &= U((U^TU)^{-1}U^TZ - \hat{D}_rV^T) + (P_U^\perp ZV(V^TV)^{-1} + U\hat{D}_r)V^T - Z \\ &= P_UZ + P_U^\perp ZP_V - P_UZ - P_U^\perp Z = P_U^\perp ZP_V - P_U^\perp Z. \end{aligned}$$

Hence, we can write

$$R(D_U, D_V) = -P_U^\perp ZP_V^\perp \quad \text{and} \quad (1/2)\|R(D_U, D_V)\|_F^2 = (1/2)\|P_U^\perp ZP_V^\perp\|_F^2. \tag{63}$$

The last term $(1/2)\|P_U^\perp ZP_V^\perp\|_F^2$ is the optimal value of (11). □

A.2 The proof of Lemma 2: Descent property of GN algorithm

Let us define $U(\alpha) := U + \alpha D_U$ and $V(\alpha) := V + \alpha D_V$ for $\alpha > 0$. Then

$$U(\alpha)V(\alpha)^T = UV^T + \alpha(UD_V^T + D_U V^T) + \alpha^2 D_U D_V^T. \tag{64}$$

Let $W := UD_V^T + D_U V^T$ and $r(\alpha) := \|U(\alpha)V(\alpha)^T - UV^T - Z\|_F^2$. Using (64) we have

$$\begin{aligned} r(\alpha) &= \|\alpha(UD_V^T + D_U V^T) + \alpha^2 D_U D_V^T - Z\|_F^2 \\ &= \|Z\|_F^2 + \alpha^2\|W\|_F^2 + \alpha^4\|D_U D_V^T\|_F^2 + 2\alpha^3\langle W, D_U D_V^T\rangle - 2\alpha\langle W, Z\rangle - 2\alpha^2\langle Z, D_U D_V^T\rangle. \end{aligned}$$

Now, using the fact that

$$\langle W, Z - W\rangle = \langle UD_V^T + D_U V^T, P_U^\perp Z P_V^\perp\rangle = \operatorname{trace}\Big((D_V U^T + V D_U^T)P_U^\perp Z P_V^\perp\Big) = 0.$$

we can further expand $r(\alpha)$ as

$$\begin{aligned} r(\alpha) &= \|Z\|_F^2 - \alpha(2-\alpha)\|W\|_F^2 + \alpha^4\|D_U D_V^T\|_F^2 \\ &\quad - 2\alpha^2(1-\alpha)\langle W, D_U D_V^T\rangle + 2\alpha^2\langle W - Z, D_U D_V^T\rangle. \end{aligned} \tag{65}$$

Using the pseudo-inverse of U and V and $(V^T)^\dagger U^\dagger = (UV^T)^\dagger$, we can show that

$$D_U D_V^T = \big(\mathbb{I}_m - 0.5P_U\big)Z(UV^T)^\dagger Z\big(\mathbb{I}_n - 0.5P_V\big).$$

From the optimality condition (6) and the definition of $Z = -L^{-1}\mathcal{A}^*\nabla\phi(\mathcal{A}(UV^T) - B))$, we can show that $\nabla_U\Phi(U,V) = -LU^T Z$ and $\nabla_V\Phi(U,V) = -LZV$. However, since D_U and D_V are given by (14), we express

$$\begin{aligned} D_U &= -\tfrac{1}{L}\big(P_U^\perp + \tfrac{1}{2}P_U\big)\nabla_U\Phi(U,V)(V^TV)^{-1} \quad \text{and} \\ D_V^T &= -\tfrac{1}{L}(U^TU)^{-1}\nabla_V\Phi(U,V)\big(P_V^\perp + \tfrac{1}{2}P_V\big). \end{aligned}$$

Using this expression, we can write $\nu := \|D_U\|_F^2 + \|D_V\|_F^2$ as

$$\nu = \frac{1}{L^2}\|\big(P_U^\perp + \frac{1}{2}P_U\big)\nabla_U\Phi(U,V)(V^TV)^{-1}\|_F^2 + \frac{1}{L^2}\|(U^TU)^{-1}\nabla_V\Phi(U,V)\big(P_V^\perp + \frac{1}{2}P_V\big)\|_F^2.$$

Hence, we can estimate

$$\frac{\|\nabla_U\Phi(U,V)\|_F^2}{4L^2(\sigma_{\max}(V))^4} + \frac{\|\nabla_V\Phi(U,V)\|_F^2}{4L^2(\sigma_{\max}(U))^4} \le \nu \le \frac{\|\nabla_U\Phi(U,V)\|_F^2}{L^2(\sigma_{\min}(U))^4} + \frac{\|\nabla_V\Phi(U,V)\|_F^2}{L^2(\sigma_{\min}(V))^4}, \tag{66}$$

where $\sigma_{\min}(\cdot)$ and $\sigma_{\max}(\cdot)$ are the smallest and largest singular values of $(\cdot)$, respectively. Let $\sigma_{\max} := \max\{\sigma_{\max}(U), \sigma_{\max}(V)\}$ and $\sigma_{\min} := \min\{\sigma_{\min}(U), \sigma_{\min}(V)\}$. Using $\|\nabla\Phi(U,V)\|_F^2 = \|\nabla_U\Phi(U,V)\|_F^2 + \|\nabla_V\Phi(U,V)\|_F^2$, (66) leads to

$$\frac{\|\nabla\Phi(U,V)\|_F^2}{4L^2\sigma_{\max}^4} \le \nu = \|D_U\|_F^2 + \|D_V\|_F^2 \le \frac{\|\nabla\Phi(U,V)\|_F^2}{L^2\sigma_{\min}^4}. \tag{67}$$

Next, using the orthonormality, we estimate $\|W\|_F^2$ as follows:

$$\begin{aligned} \|W\|_F^2 &= \|UD_V^T + D_U V^T\|_F^2 = \|UD_V^T\|_F^2 + \|D_U V^T\|_F^2 \\ &= \operatorname{trace}\Big(D_V(U^TU)D_V^T\Big) + \operatorname{trace}\Big(D_U(V^TV)D_U^T\Big) \\ &\ge (\sigma_{\min}(U))^2\|D_U\|_F^2 + (\sigma_{\min}(V))^2\|D_V\|_F^2 \ge \sigma_{\min}^2\nu. \end{aligned} \tag{68}$$

On the one hand, we estimate individually each term of the expression (65) as follows:

$$\|D_U D_V^T\|_F^2 = \operatorname{trace}\Big((D_U D_V^T)^T(D_U D_V)\Big) \le \frac{1}{4}\left(\|D_U\|_F^2 + \|D_V\|_F^2\right)^2 = \frac{\nu^2}{4}.$$

On the other hand, since $W - Z = -P_U^{\perp} Z P_V^{\perp}$ by Lemma 1, we can show that

$$\langle W - Z, D_U D_V^T\rangle = \langle P_U^{\perp} Z P_V^{\perp}, D_U D_V^T\rangle = \mathrm{trace}\left(D_V^T P_V^{\perp} Z^T P_U^{\perp} D_U\right) \le \|Z\|_F \|D_U D_V^T\|_F.$$

In addition, $-\langle W, D_U D_V\rangle \le \|W\|_F\|D_U D_V^T\|_F$. Substituting these estimates into (65) and using the fact that $2-\alpha \ge 1$ and $1-\alpha \le 1$ we obtain

$$\begin{aligned}
r(\alpha) &\le \|Z\|_F^2 - \alpha\|W\|_F^2 + \frac{\nu^2\alpha^4}{4} + 2\alpha^2\|W\|_F\|D_U D_V^T\|_F + 2\alpha^2\|Z\|_F\|D_U D_V^T\|_F\\
&\le \|Z\|_F^2 - \frac{\alpha}{16}\|W\|_F^2 - \frac{\alpha\nu\sigma_{\min}^2}{16} + \frac{\nu^2\alpha^4}{4} - \frac{\alpha}{2}\|W\|_F^2 + 2\alpha^2\|W\|_F\|D_U D_V^T\|_F\\
&- \frac{3\alpha}{8}\|W\|_F^2 + 2\alpha^2\|Z\|_F\|D_U D_V^T\|_F\\
&= \|Z\|_F^2 - \frac{\alpha\nu\sigma_{\min}^2}{16} - \frac{\alpha\nu}{16}\left(\sigma_{\min}^2 - 4\alpha^3\nu\right)_{[b_1]} - \frac{\alpha}{2}\|W\|_F\Big(\|W\|_F - 4\alpha\|D_U D_V^T\|_F\Big)_{[b_2]}\\
&- \frac{\alpha}{8}\Big(3\|W\|_F^2 - 16\alpha\,\|Z\|_F\left\|D_U D_V^T\right\|_F\Big)_{[b_3]}\\
&= \|Z\|_F^2 - \frac{\alpha\nu\sigma_{\min}^2}{16} - \frac{\alpha\nu}{16}b_1 - \frac{\alpha}{2}\|W\|_F b_2 - \frac{\alpha}{8}b_3.
\end{aligned} \tag{69}$$

We estimate each term in (69). From (68), we can see that $W = 0$ implies $D_U = 0$ and $D_V = 0$, which is contradict to our assumption. Hence, $W \neq 0$. First, we choose $\alpha \in (0, 1]$ such that

$$\sigma_{\min}^2 \ge \left(\frac{16\|Z\|_F}{3\|W\|_F}\right)^2 \nu\alpha^2 \quad \text{and} \quad \sigma_{\min}^2 \ge 4\nu\alpha^2. \tag{70}$$

Since $W \neq 0$, this condition allows us to compute α as

$$0 < \alpha \le \frac{\sigma_{\min}}{2\sqrt{\nu}}\min\left\{1, \frac{3\|W\|_F}{8\|Z\|_F}\right\}. \tag{71}$$

Under the second condition of (70) and $\alpha \in (0, 1]$, we have $b_1 = \sigma_{\min}^2 - 4\nu\alpha^3 \ge \sigma_{\min}^2 - 4\nu\alpha^2 \ge 0$. Next, since (68) and the first condition in (70) we have $\sigma_{\min}^2 \ge 4\alpha^2\nu$. Using (68) we have $\|W\|_F^2 \ge \sigma_{\min}^2\nu \ge 4\alpha^2\nu^2 = 4\alpha^2\big(\|D_U\|_F^2 + \|D_V\|_F^2\big)^2 \ge 16\alpha^2\left\|D_U D_V^T\right\|_F^2$. Hence, $\|W\|_F \ge 4\alpha\left\|D_U D_V^T\right\|_F$. Using this inequality, we can estimate $b_2 = \|W\|_F - 4\alpha\|D_U D_V^T\|_F \ge 0$.

Then, using $\|W\|_F^2 \ge \sigma_{\min}^2\nu \ge \left(\frac{16\|Z\|_F}{3\|W\|_F}\right)^2\alpha^2\nu^2$, we have $\|W\|_F \ge \frac{16\|Z\|_F}{3\|W\|_F}\nu\alpha$. Therefore, we can estimate

$$b_3 = 3\|W\|_F^2 - 16\alpha\|Z\|_F\|D_U D_V^T\|_F \ge 3\alpha\|W\|_F\frac{16\|Z\|_F}{3\|W\|_F} - 16\alpha\|Z\|_F\|D_U D_V^T\|_F = 0.$$

From (67) we have $\sqrt{\nu} \le \frac{\|\nabla\Phi(U,V)\|_F}{L\sigma_{\min}^2}$, while from (68) we have $\|W\|_F \ge \sqrt{\nu}\sigma_{\min} \ge \frac{\sigma_{\min}\|\nabla\Phi(U,V)\|_F}{2L\sigma_{\max}^2}$. Substituting these estimates into (71) of α and using $\|Z\|_F = \frac{1}{L}\left\|\nabla\phi(\mathcal{A}(UV^T) - M)\right\|_F = \frac{1}{L}\left\|\Phi'(UV^T)\right\|_F$ we can lower estimate α as

$$0 < \alpha \le \frac{\sigma_{\min}^3 L}{2\|\nabla\Phi(U,V)\|_F}\min\left\{1, \frac{3\sigma_{\min}\|\nabla\Phi(U,V)\|_F}{16L\|\Phi'(UV^T)\|_F\sigma_{\max}^2}\right\}. \tag{72}$$

Note that $\alpha \in (0, 1]$, we obtain from (72) the update rule (16).

We finally estimate (17). Since α satisfies (16), it follows from (69) that

$$r(\alpha) \le \|Z\|_F^2 - \frac{\alpha\nu\sigma_{\min}^2}{16} \overset{(67)}{\le} \|Z\|_F^2 - \frac{\alpha\sigma_{\min}^2}{64L^2\sigma_{\max}^4}\|\nabla\Phi(U,V)\|^2$$

Substituting this inequality into (8) we obtain (17). □.

A.3 The proof of Lemma 3: Full-rankness of iterates

Since $\mathrm{rank}\,(U) = \mathrm{rank}\,(V) = r$ by assumption, we have $\lambda_{\min}(U^TU) > 0$ and $\lambda_{\min}(V^TV) > 0$. We consider $Q := (U^\dagger)^T = U(U^TU)^{-1}$ and $S := (V^\dagger)^T = V(V^TV)^{-1}$. We always have $U_+^T(\lambda_{\max}(QQ^T)\mathbb{I} - QQ^T)U_+ \succeq 0$. This implies that

$$\lambda_{\min}(U_+^TU_+)\lambda_{\max}(QQ^T) \geq \lambda_{\min}((Q^TU_+)^T(Q^TU_+)).$$

Clearly, since $Q^T = U^\dagger$, we have $\lambda_{\max}(QQ^T) = \lambda_{\min}^{-1}(U^TU)$. Using this into the last inequality, we get

$$\frac{\lambda_{\min}(U_+^TU_+)}{\lambda_{\min}(U^TU)} \geq \lambda_{\min}((Q^TU_+)^T(Q^TU_+)). \tag{73}$$

Hence, it is sufficient to show that $\lambda_{\min}((Q^TU_+)^T(Q^TU_+)) > 0$. By Lemma 1, we have $U_+ = U + \alpha D_U = U + \alpha(P_U^\perp + 0.5P_U)ZV(V^TV)^{-1}$. Therefore, we can compute $Q^TU_+ = \mathbb{I}_m + 0.5\alpha H$, where $H := (U^TU)^{-1}U^TZV(V^TV)^{-1}$. Then, we estimate $\lambda_{\min}((Q^TU_+)^T(Q^TU_+))$ as follows:

$$\begin{aligned}
\lambda_{\min}((Q^TU_+)^T(Q^TU_+)) &= \lambda_{\min}\left(\mathbb{I} + 0.5\alpha(H^T + H) + \alpha^2H^TH\right)\\
&\overset{[1,\ 9.13.6.]}{\geq} 1 - 0.5\alpha\lambda_{\max}(H^T + H) \overset{[1,\ 5.11.25]}{\geq} 1 - \alpha\sigma_{\max}(H)\\
&= 1 - \alpha\sigma_{\max}\left((U^TU)^{-1}U^TZV(V^TV)^{-1}\right)\\
&\geq 1 - \frac{\alpha\sigma_{\max}(U^TZ)}{\sigma_{\min}(U)^2\sigma_{\min}(V)} \geq 1 - \frac{\alpha\|U^TZ\|_F}{\sigma_{\min}^3},
\end{aligned}$$

where $\sigma_{\min} = \min\{\sigma_{\min}(U), \sigma_{\min}(V)\}$ and $\|U^TZ\|_F \geq \sigma_{\max}(U^TZ)$. We note that $\|\Phi(U,V)\|_F \geq \|\nabla_U\Phi(U,V)\|_F = L\|U^TZ\|$. Substituting this estimate into the last inequality and noting from (16) that $\alpha \leq \frac{\sigma_{\min}^3L}{2\|\nabla\Phi(U,V)\|_F}$, we obtain

$$\lambda_{\min}((Q^TU_+)^T(Q^TU_+)) \geq 1 - \alpha\frac{\|\nabla\Phi(U,V)\|_F}{L\sigma_{\min}^3} \geq 1 - \frac{L}{2L} = \frac{1}{2} > 0.$$

Combining this estimate and (73) we have $\lambda_{\min}(U_+^TU_+) \geq 0.5\lambda_{\min}(U^TU)$. Hence, we conclude that $\mathrm{rank}\,(U_+) = r$. With a similar proof, we can show $\mathrm{rank}\,(V_+) = r$. □

A.4 The proof of Theorem 1: Global convergence of GN method

By Lemma 2, we can see that the backtracking linesearch step at Step 6 of Algorithm 1 is finite and $\alpha_k > 0$. The inequality (19) guarantees that $\Phi(U_{k+1}, V_{k+1}) < \Phi(U_k, V_k)$. Hence, the sequence $\{\Phi(U_k, V_k)\}$ is decreasing and bounded from below by $\Phi^\star$. It converges to a limit point Φ^*. Now, using (19) we obtain

$$\sum_{k=0}^{n}\alpha_k\|\nabla\Phi(U_k,V_k)\|_F^2 \leq \Phi(U_0,V_0) - \Phi(U_{n+1},V_{n+1}) \leq \Phi(U_0,V_0) - \Phi^\star < +\infty.$$

Taking the limit in this inequality as $n \to \infty$, we obtain $\sum_{k=0}^{\infty}\alpha_k\|\nabla\Phi(U_k,V_k)\|_F^2 < +\infty$. Consequently, $\lim_{k\to\infty}\alpha_k\|\nabla\Phi(U_k,V_k)\|_F^2 = 0$. This proves the first part (22).

In order to prove the second part, we need to show that $\alpha_k \geq \alpha > 0$ for all k sufficiently large. Indeed, by our assumption $\{[U_k, V_k]\}$ is bounded. Hence, $\|\Phi'(U_k,V_k)\|_F \leq K_1 < +\infty$.Similarly, $\|\nabla\Phi(U_k,V_k)\|_F \leq K_2 < +\infty$ and $\max\{\sigma_{\max}(U_k), \sigma_{\max}(V_k)\} \leq K_3 < +\infty$.Using these arguments and condition (21) into (16), we obtain

$$2\alpha_k \geq \underline{\alpha} \overset{(16)}{\geq} 2\alpha := \min\left\{1, \frac{L\underline{\sigma}^3}{2K_2}, \frac{3\underline{\sigma}^4}{32K_1K_3^2}\right\} > 0.$$

Using this into (22) we have $\lim_{k\to\infty}\|\nabla\Phi(U_k,V_k)\|_F^2 \leq \alpha^{-1}\lim_{k\to\infty}\alpha_k\|\nabla\Phi(U_k,V_k)\|_F^2 = 0$, which implies (23).

By our assumption, $\{X_k\}$ generated by Algorithm 1 is bounded. Hence, there exists a limit point $X_\star := [U_\star, V_\star]$. Passing the limit (23) via subsequence, we can see that $\nabla\Phi(U_\star, V_\star) = 0$, and hence, $X_\star$ satisfies the optimality condition (6). □

A.5 The proof of Lemma 4: Descent property of $\mathcal{L}_\rho$

We first prove part (a). The boundedness of $\{[U_k, V_k]\}$ follows directly from Assumption A.21. Since $\lim_{k\to\infty}\|W_k - \mathcal{A}(U_kV_k^T) + B\|_F = 0$ due to part (b), $\{W_k\}$ is also bounded.

Now, we prove part (b) for **Option 1**. First, since $[U_{k+1}, V_{k+1}]$ is updated by Step 5 of Algorithm 2 that satisfies the backtracking linesearch condition (35), we have

$$\mathcal{Q}_k(U_{k+1}, V_{k+1}) \le \mathcal{Q}_k(U_k, V_k) - 0.5c_1\alpha_k\Delta_k^2, \tag{74}$$

where $\mathcal{Q}_k$ is defined by (35), $E_k := \mathcal{A}(U_kV_k^T) - B + \rho^{-1}\Lambda_k$, and Δ_k^2 is

$$\Delta_k^2 := \|U_k^T\mathcal{A}^*(E_k - W_k)\|_F^2 + \|\mathcal{A}^*(E_k - W_k)V_k\|_F^2. \tag{75}$$

This condition implies

$$\mathcal{L}_\rho(U_{k+1}, V_{k+1}, W_k, \Lambda_k) \le \mathcal{L}_\rho(U_k, V_k, W_k, \Lambda_k) - \frac{c_1\rho\alpha_k}{2}\Delta_k^2. \tag{76}$$

Second, we consider the objective function $h(W) := \phi(W) + (\rho/2)\|W - C_k\|_F^2$ of (28b), where $C_k := \mathcal{A}(U_{k+1}V_{k+1}) - B + \rho^{-1}\Lambda_k$. Since $h(\cdot)$ is strongly convex with the strong convexity parameter $\rho + \mu_\phi$, and W_{k+1} is the optimal solution of h, we have

$$h(W_{k+1}) \le h(W_k) - ((\rho + \mu_\phi)/2)\|W_{k+1} - W_k\|_F^2.$$

Using this inequality, the definitions of h and $\mathcal{L}_\rho$, we can show that

$$\mathcal{L}_\rho(U_{k+1}, V_{k+1}, W_{k+1}, \Lambda_k) \le \mathcal{L}_\rho(U_{k+1}, V_{k+1}, W_k, \Lambda_k) - \frac{(\rho + \mu_\phi)}{2}\|W_{k+1} - W_k\|_F^2. \tag{77}$$

In addition, since ϕ is L_ϕ-smooth, we can write down the optimality condition of (28b) as $\nabla\phi(W_{k+1}) + \rho(W_{k+1} - C_k) = 0$. Using the definition of C_k and (28c) we get $\Lambda_{k+1} = \nabla\phi(W_{k+1})$. Hence, we can derive

$$\|\Lambda_{k+1} - \Lambda_k\|_F = \|\nabla\phi(W_{k+1}) - \nabla\phi(W_k)\|_F \le L_\phi\|W_{k+1} - W_k\|_F, \tag{78}$$

which is the first inequality in (37).

Third, since Λ_k is updated by (28c), using the definition of $\mathcal{L}_\rho$, it is easy to show

$$\begin{aligned}\mathcal{L}_\rho(U_{k+1}, V_{k+1}, W_{k+1}, \Lambda_{k+1}) &= \mathcal{L}_\rho(U_{k+1}, V_{k+1}, W_{k+1}, \Lambda_k) + \rho^{-1}\|\Lambda_{k+1} - \Lambda_k\|_F^2\\ &\overset{(78)}{\le} \mathcal{L}_\rho(U_{k+1}, V_{k+1}, W_{k+1}, \Lambda_k) + \rho^{-1}L_\phi^2\|W_{k+1} - W_k\|_F^2.\end{aligned} \tag{79}$$

Summing up (76), (77) and (79) we get (38).

Finally, we prove (b) for **Option 2**. We consider the gradient step (33) instead of (28b). Using the optimality condition of (32) and (28c), we can derive $\Lambda_{k+1} = \nabla\phi(W_k) + L_\phi(W_{k+1} - W_k)$. Using this and the Lipschitz continuity of $\nabla\phi$, we have

$$\begin{aligned}\|\Lambda_{k+1} - \Lambda_k\|_F &= \|L_\phi(W_{k+1} - W_{k-1}) + \nabla\phi(W_k) - \nabla\phi(W_{k-1})\|_F\\ &\le L_\phi\big[\|W_{k+1} - W_{k-1}\|_F + \|W_k - W_{k-1}\|_F\big],\end{aligned} \tag{80}$$

which is exactly the second expression of (37). Now, since we apply the gradient step to solve (28b), with h defined as in (77), it is well-known that

$$h(W_{k+1}) \le h(W_k) - ((L_\phi + \rho)/2)\|W_{k+1} - W_k\|_F^2,$$

which implies

$$\mathcal{L}_\rho(U_{k+1}, V_{k+1}, W_{k+1}, \Lambda_k) \le \mathcal{L}_\rho(U_{k+1}, V_{k+1}, W_k, \Lambda_k) - \frac{(\rho + L_\phi)}{2}\|W_{k+1} - W_k\|_F^2. \tag{81}$$

Summing up (76), (81) and the first equality of (79) we obtain

$$\mathcal{L}_\rho(U_{k+1}, V_{k+1}, W_{k+1}, \Lambda_{k+1}) = \mathcal{L}_\rho(U_k, V_k, W_k, \Lambda_k) - (1/2)c_1\rho\alpha_k\Delta_k^2 - T_k, \tag{82}$$

where $T_k := \frac{(\rho+L_\phi)}{2}\|W_{k+1}-W_k\|_F^2 - \rho^{-1}\|\Lambda_{k+1}-\Lambda_k\|_F^2$. Finally, using (80), we can estimate $\|\Lambda_{k+1}-\Lambda_k\|_F$ as follows:

$$\begin{aligned}\|\Lambda_{k+1}-\Lambda_k\|_F^2 &\le L_\phi^2\big[\|W_{k+1}-W_{k-1}\|_F + \|W_k - W_{k-1}\|_F\big]^2\\ &\le 2L_\phi^2\|W_{k+1}-W_k\|_F^2 + 4L_\phi^2\|W_k-W_{k-1}\|_F^2.\end{aligned}$$

Hence, $T_k \ge (0.5(\rho+L_\phi) - 2\rho^{-1}L_\phi^2)\|W_{k+1}-W_k\|_F^2 - 4\rho^{-1}L_\phi^2\|W_k-W_{k-1}\|_F^2$. Substituting this estimate of T_k into (82) we obtain (38). □

A.6 The proof of Theorem 3: Global convergence of GN-ADMM

We first prove for **Option 1**. Let us define $\eta := \rho^{-1}(\rho^2 + \mu_\phi\rho - 2L_\phi^2)$. Then $\eta > 0$ if we choose $\rho > 0.5((\mu_\phi + 8L_\phi^2)^{1/2} + \mu_\phi)$ as given by (39) in Lemma 4. Hence, the sequence $\{\mathcal{L}_\rho(U_k, V_k, W_k, \Lambda_k)\}$ is strictly decreasing, it is bounded from bellow due to Assumption A.21. It converges to a finite value $\mathcal{L}_\rho^\star$. In addition, (38) implies

$$\begin{aligned}&\lim_{k\to\infty}\|W_{k+1}-W_k\|_F = 0,\\ &\lim_{k\to\infty}\alpha_k\big\|U_k^T\mathcal{A}^*\big(\rho^{-1}\Lambda_k + \mathcal{A}(U_kV_k^T) - B - W_k\big)\big\|_F^2 = 0, \quad\text{and}\\ &\lim_{k\to\infty}\alpha_k\big\|\mathcal{A}^*\big(\rho^{-1}\Lambda_k + \mathcal{A}(U_kV_k^T) - B - W_k\big)V_k\big\|_F^2 = 0.\end{aligned} \tag{83}$$

Under condition (21), as in the proof of Theorem 1 we can show that $\alpha_k \ge 0.5\underline{\alpha} > 0$ for k sufficiently large. Hence, the two last limits of (83) imply

$$\begin{aligned}&\lim_{k\to\infty}\big\|U_k^T\mathcal{A}^*\big(\Lambda_k + \rho\big(\mathcal{A}(U_kV_k^T) - B - W_k\big)\big)\big\|_F = 0 \text{ and}\\ &\lim_{k\to\infty}\big\|\mathcal{A}^*\big(\Lambda_k + \rho\big(\mathcal{A}(U_kV_k^T) - B - W_k\big)V_k\big\|_F = 0.\end{aligned} \tag{84}$$

On the other hand, using Lemma 4(a), (28c) and the first limit in (83), we obtain

$$\begin{aligned}\lim_{k\to\infty}\|\mathcal{A}(U_{k+1}V_{k+1}^T) - W_{k+1} - B\|_F &\overset{(28c)}{=} \rho^{-1}\lim_{k\to\infty}\|\Lambda_{k+1}-\Lambda_k\|_F\\ &\overset{\text{Lemma A.5(a)}}{\le} \rho^{-1}L_\phi\lim_{k\to\infty}\|W_{k+1}-W_k\|_F \overset{(83)}{=} 0.\end{aligned} \tag{85}$$

We consider a convergent subsequence $\big\{[U_{k_i}, V_{k_i}]\big\}_{i\in\mathbb{N}}$ with the limit $[U_*, V_*]$. Then, the limit (85) shows that the corresponding subsequence $\big\{W_{k_i}\big\}$ also converges to W_* such that $W_* = \mathcal{A}(U_*V_*^T) - B$, which is the last condition in (36).

Now, using the limit in (85) and combining with the triangle inequality, we get

$$\begin{aligned}\|U_k^T\mathcal{A}^*(\Lambda_k)\|_F &\le \big\|U_k^T\mathcal{A}^*\big(\Lambda_k + \rho\big(\mathcal{A}(U_kV_k^T) - B - W_k\big)\big)\big\|_F\\ &\quad + \rho\big\|U_k^T\mathcal{A}^*\big(\mathcal{A}(U_kV_k^T) - B - W_k\big)\big\|_F \overset{(84),(85)}{\to} 0 \;\text{ as }\; k_i\to\infty.\end{aligned}$$

This implies $U_*^T\mathcal{A}^*(\Lambda_*) = 0$ via subsequence. Similarly, we can also show that $\mathcal{A}^*(\Lambda_*)V_* = 0$. These are the second and the third condition in (36). Finally, the first condition of (36) follows directly from the relation $\Lambda_k = \nabla\phi(W_k)$ as the optimality condition of (28b) by taking the limit via subsequence.

We have shown in the above steps that the limit point $(U_*, V_*, W_*, \Lambda_*)$ satisfies the optimality condition (36) of (26). By eliminating Λ_* and W_* in (36) we obtain (6), which shows that any limit point $[U_*, V_*]$ of $\{[U_k, V_k]\}$ is a stationary point of (1). The proof of (41) can be done as in Theorem 1.

We prove for **Option 2**. We note that if $\rho > 3L_\phi$, then we can examine from (39) that $\eta_1 > \eta_0$. If we denote by $\mathcal{L}_k := \mathcal{L}_\rho(U_k, V_k, W_k, \Lambda_k)$ and $r_k := \|W_k - W_{k-1}\|_F$ for $k \ge 1$, then we can write (38) as

$$\mathcal{L}_{k+1} + \frac{\eta_0}{2}r_{k+1}^2 \le \mathcal{L}_k + \frac{\eta_0}{2}r_k^2 - \frac{c_1\rho}{2}\Delta_k^2 - \frac{(\eta_1-\eta_0)}{2}r_{k+1}^2.$$

By induction, we can show from this inequality that $\sum_{k=0}^{\infty}\Big(c_1\rho\Delta_k^2 + (\eta_1-\eta_0)r_{k+1}^2\Big) = 0$, which implies (83). With the same proof as in **Option 1** we obtain the same conclusions of the theorem as in **Option 1**. □

A.7 The proof of Theorem 2: Local convergence of GN method

Let $x := [\mathrm{vec}\,(U), \mathrm{vec}\,(V^T)] \in \mathbb{R}^{(m+n)r}$ be the vecterization of U and V, and $R(x) := \mathcal{A}(UV^T) - B$ be the residual term. We can compute the Jacobian $J_R(x)$ of R at x as $J_R(x) = A[V \otimes \mathbb{I}_m, \mathbb{I}_n \otimes U^T] \in \mathbb{R}^{l\times(m+n)r}$, where A is the matrix form of the linear operator $\mathcal{A}$. The objective function $\Phi(U,V)$ can be written as $\Phi(x) = \phi(R(x))$. Its gradient and Hessian are given by the following forms:

$$\begin{aligned}\nabla\Phi(x) &= J_R(x)^T\nabla\phi(R(x)) \ \text{ and}\\ \nabla^2\Phi(x) &= J_R(x)^T\nabla^2\phi(R(x))J_R(x) + \sum_{i=1}^{l}\frac{\partial\phi(R(x))}{\partial R_i}\nabla^2 R_i(x).\end{aligned} \tag{86}$$

First, we show that under Assumption A.31(a), $\nabla^2\Phi$ is also Lipschitz continuous in $\mathcal{N}(x_\star)$ of $x_\star \in \mathcal{X}_\star$. Indeed, $\nabla^2 R(x)$ is bounded in $\mathcal{N}(x_\star)$ by $M_{R_i''}$, and $\nabla^2 R_i(\cdot)$ is Lipschitz continuous with the Lipschitz constant $L_{R_i''}$. In addition, $J_R(\cdot)$ is also bounded in $\mathcal{N}(x_\star)$ by $M_{R'}$, and R is also Lipschitz continuous with the Lipschitz constant L_R. Since $\nabla^2\phi$ is Lipschitz continuous in $\mathcal{N}(R(x_\star))$, then $\frac{\partial\phi(R(x)}{\partial R_i}$ is also bounded by $M^i_{\phi'}$, and Lipschitz continuous in $\mathcal{N}(R(x_\star))$ with the Lipschitz constant $L^i_{\phi'}$. Combining these statements and (86), we can show that for any $x, \hat{x} \in \mathcal{N}(x_\star)$:

$$\begin{aligned}\|\nabla^2\Phi(x) - \nabla^2\Phi(\hat{x})\| &\le \Big\|J_R(x)^T\nabla^2\phi(R(x))J_R(x) - J_R(\hat{x})^T\nabla^2\phi(R(\hat{x}))J_R(\hat{x})\Big\|\\
&+ \left\|\sum_{i=1}^{l}\left[\frac{\partial\phi(R(x))}{\partial R_i}\nabla^2 R_i(x) - \frac{\partial\phi(R(\hat{x}))}{\partial R_i}\nabla^2 R_i(\hat{x})\right]\right\|\\
&\le \Big\|J_R(x)^T\nabla^2\phi(R(x))\left(J_R(x) - J_R(\hat{x})\right)\Big\|\\
&+ \Big\|J_R(x)^T\left(\nabla^2\phi(R(x)) - \nabla^2\phi(R(\hat{x}))\right)J_R(\hat{x})\Big\|\\
&+ \Big\|\left(J_R(x) - J_R(\hat{x})\right)^T\nabla^2\phi(R(\hat{x}))J_R(\hat{x})\Big\|\\
&+ \sum_{i=1}^{l}\Big[\Big\|\frac{\partial\phi(R(x))}{\partial R_i}\left(\nabla^2 R_i(x) - \nabla^2 R_i(\hat{x})\right)\Big\|\\
&+ \Big\|\left(\frac{\partial\phi(R(x))}{\partial R_i} - \frac{\partial\phi(R(\hat{x}))}{\partial R_i}\right)\nabla^2 R_i(\hat{x})\Big\|\Big]\\
&\le \Big(2M_{R'}M_{\phi''}L_{R'} + M^2_{R'}L_{\phi''} + \sum_{i=1}^{l}(M_{R_i''}L^i_{\phi'} + L_{R_i''}M^i_{\phi'})\Big)\|x - \hat{x}\|.\end{aligned}$$

This inequality shows that $\nabla\Phi$ is Lipschitz continuous in $\mathcal{N}(x_\star)$ with the Lipschitz constant $L_{\Phi''} := 2M_{R'}M_{\phi''}L_{R'} + M^2_{R'}L_{\phi''} + \sum_{i=1}^{l}(M_{R_i''}L^i_{\phi'} + L_{R_i''}M^i_{\phi'}) > 0$.

Next, we consider the GN direction D_{X_k} in (11). Let $d := [\mathrm{vec}\,(D_U), \mathrm{vec}\,(D_V^T)]$ and $H_0(x) := \begin{bmatrix} V^T\otimes U & V^TV\otimes\mathbb{I}_m\\ \mathbb{I}_n\otimes U^TU & V\otimes U^T\end{bmatrix}$. Due to the full-rankness of U and V, by using the result in [8] we can show that $H_0(x)^\dagger$ is bounded by M_h, i.e.:

$$\|H_0(x)^\dagger\| \le M_h < +\infty. \tag{87}$$

Moreover, we can see from (12) that $[\mathrm{vec}\,(ZV), \mathrm{vec}\,(U^TZ)] = -L^{-1}J_R(x)^T\nabla\phi(R(x))$. Hence, (12) can be written as $H_0(x)d = -L^{-1}J_R(x)^T\nabla\phi(R(x))$, which implies $d = -L^{-1}H_0(x)^\dagger\nabla\Phi(x)$. The full-step GN scheme becomes

$$x_+ = x + d = x - L^{-1}H_0(x)^\dagger\nabla\Phi(x). \tag{88}$$

We consider the residual term $r = x - x_\star$, where $x_\star := [\mathrm{vec}\,(U_\star)\,, \mathrm{vec}\,(V_\star^T)] \in \mathcal{X}_\star$ is a given stationary point of (1). From (88) we can write

$$\begin{aligned} r_+ = x_+ - x_\star &= r - L^{-1}H_0(x)^\dagger\nabla\Phi(x) = r - L^{-1}H_0(x)^\dagger\left[\nabla\Phi(x) - \nabla\Phi(x_\star)\right] \\ &= \left[\mathbb{I} - L^{-1}H_0(x)^\dagger\nabla^2\Phi(x_\star)\right] r \\ &- L^{-1}H_0(x)^\dagger\left[\int_0^1 \left(\nabla^2\Phi(x_\star+\tau(x-x_\star)) - \nabla^2\Phi(x_\star)\right)(x-x_\star)d\tau\right]. \end{aligned}$$

Using condition (24) and the Lipschitz continuity of $\nabla\Phi$, this expression leads to

$$\begin{aligned} \|r_+\| &\le \|\left(\mathbb{I} - L^{-1}H_0(x)^\dagger\nabla^2\Phi(x_\star)\right) r\| \\ &+ L^{-1}\|H_0(x)^\dagger\|\int_0^1 \|\nabla^2\Phi(x_\star+\tau(x-x_\star)) - \nabla^2\Phi(x_\star)\|\|x-x_\star\|d\tau \\ &\le \kappa(x_\star)\|r\| + \frac{1}{2}L^{-1}L_{\Phi''}\|H_0(x)^\dagger\|\|r\|^2 \\ &\le \left(\bar{\kappa} + 0.5L^{-1}L_{\Phi''}K_h\|r\|\right)\|r\|. \end{aligned} \tag{89}$$

Since $r = x - x_\star = \mathrm{vec}\,(X - X_\star)$, we can write (89) as

$$\|X_+ - X_\star\|_F \le \left(\bar{\kappa} + 0.5L^{-1}L_{\Phi''}K_h\|X - X_\star\|_F\right)\|X - X_\star\|_F,$$

which is exactly (25) with $K_1 := L^{-1}L_{\Phi''}K_h > 0$.

Next, we prove quadratic convergence of the full-step GN scheme. Under Assumption 21, it follows from [18] that there exists a neighborhood $\mathcal{N}(x_\star)$ of $x_\star$ such that $H_0(\cdot)^\dagger$ is Lipschitz continuous in $\mathcal{N}(x_\star$ with the Lipschitz constant $L_H > 0$. Here, we use the same $\mathcal{N}(x_\star$ as in Assumption 31. Otherwise, we can shrink it if necessary. We consider the condition $H(X_\star)^\dagger\nabla^2\Phi(X_\star) = L\mathbb{I}$. Reforming this condition into vector form, we have $H_0(x_\star)^\dagger\nabla^2\Phi(x_\star) = L\mathbb{I}$, which is equivalent to $\mathbb{I} - L^{-1}H(X_\star)^\dagger\nabla^2\Phi(X_\star) = 0$. Using the last condition, and the Lipschitz continuity of $H_0^\dagger(\cdot)$, we can show that

$$\begin{aligned} S(x_\star) &:= \|\left[\mathbb{I} - L^{-1}H_0(x)^\dagger\nabla^2\Phi(x_\star)\right](x - x_\star)\| \\ &\le \|\left[\mathbb{I} - L^{-1}H_0(x_\star)^\dagger\nabla^2\Phi(x_\star)\right](x-x_\star)\| + L^{-1}\|\left(H_0(x)^\dagger - H_0(x_\star)^\dagger\right)(x-x_\star)\| \\ &\le L^{-1}\|H_0(x)^\dagger - H_0(x_\star)^\dagger\|\|x-x_\star\| \\ &\le L^{-1}L_H\|x - x_\star\|^2, \quad \forall x \in \mathcal{N}(x_\star). \end{aligned}$$

Substituting this $S(x_\star)$ estimate into (89) we get $\|r_+\| \le L^{-1}(L_H + 0.5L_{\Phi''}K_h)\|r\|^2$, which is reformed into the matrix form as

$$\|X_+ - X_\star\|_F \le 0.5K_2\|X - X_\star\|_F^2,\ \forall X \in \mathcal{N}(X_\star),\ \text{where } K_2 := L^{-1}\left(2L_H + L_{\Phi''}K_h\right).$$

In order to guarantee the monotonicity of $\{\|X - X_\star\|_F\}$, we require $\|X_+ - X_\star\|_F \le 0.5K_1\|X - X_\star\|_F^2 < \|X - X_\star\|_F$, which implies $\|X - X_\star\|_F < 2K_2^{-1}$. Hence, if we choose $X_0 \in \mathcal{N}(X_\star)$ such that $\|X_0 - X_\star\|_F < 2K_2^{-1}$, then $\|X_k - X_\star\|_F < 2K_2^{-1}$ for all k and $\{\|X_k - X_\star\|_F\}$ is monotone. Moreover, the estimate $\|X_{k+1} - X_\star\|_F \le 0.5K_2\|X_k - X_\star\|_F^2$ shows that this sequence converges quadratically to zero. Hence, $\{X_k\}$ converges to $X_\star$ at a quadratic rate. Here, we can easily check that $K_2 > K_1$.

Finally, if $\bar{\kappa} \in (0, 1)$, then the estimate (25) implies that

$$\|X_{k+1} - X_\star\|_F \le \left(\bar{\kappa} + 0.5K_1\|X_k - X_\star\|_F\right)\|X_k - X_\star\|_F,$$

for $k \ge 0$. In order to guarantee $\|X_{k+1} - X_\star\|_F < \|X_k - X_\star\|_F$, we require $\bar{\kappa} + 0.5K_1\|X_k - X_\star\|_F < 1$, which leads to $\|X_k - X_\star\|_F < 2K_1^{-1}(1 - \bar{\kappa})$. Hence, if we take $\bar{r}_0 < 2K_1^{-1}(1 - \bar{\kappa})$, and choose $X_0 \in \mathcal{N}(X_\star)$ such that $\|X_0 - X_\star\|_F \le \bar{r}_0$, then $\|X_k - X_\star\|_F \le \bar{r}_0$ for all $k \ge 0$. In addition, we have $\|X_{k+1} - X_\star\|_F \le (\bar{\kappa} + 0.5K_1\|X_k - X_\star\|_F)\|X_k - X_\star\|_F \le (\bar{\kappa} + 0.5K_1\bar{r}_0)\|X_k - X_\star\|_F$, which shows that $\{\|X_k - X_\star\|_F\}$ converges to zero at a linear rate with the contraction factor $\omega := \bar{\kappa} + 0.5K_1\bar{r}_0 < 1$. □

References

1. Bernstein, D. *Matrix mathematics*. Princeton University Press, 2005.
2. Bhojanapalli, S., Kyrillidis, A., and Sanghavi, S. Dropping convexity for faster semi-definite optimization. *arXiv preprint arXiv:1509.03917* (2015).
3. Björck, A. *Numerical Methods for Least Squares Problems*. SIAM, 1996.
4. Bottou, L. Large-scale machine learning with stochastic gradient descent. In *Proceedings of COMPSTAT'2010*. Springer, 2010, pp. 177–186.
5. Boyd, S., Parikh, N., Chu, E., Peleato, B., and Eckstein, J. Distributed optimization and statistical learning via the alternating direction method of multipliers. *Foundations and Trends in Machine Learning 3*, 1 (2011), 1–122.
6. Burer, S., and Monteiro, R. D. A nonlinear programming algorithm for solving semidefinite programs via low-rank factorization. *Math. Program. 95*, 2 (2003), 329–357.
7. Cai, J.-F., Candes, E. J., and Shen, Z. A singular value thresholding algorithm for matrix completion. *SIAM J. Optim. 20*, 4 (1956), 2010.
8. Campbell, S. L., and Meyer, C. D. *Generalized inverses of linear transformations*, vol. 56. SIAM, 2009.
9. Candés, E., Li, X., Ma, Y., and Wright, J. Robust principal component analysis? *Journal of the ACM 58*, 3 (2011), 1–37.
10. Candès, E., and Recht, B. Exact matrix completion via convex optimization. *Communications of the ACM 55*, 6 (2012), 111–119.
11. Candes, E., Romberg, J., and Tao, T. Stable signal recovery from incomplete and inaccurate measurements. *Commun. Pure Appl. Math. 8* (2006), 1207–1223.
12. Candes, E. J., Eldar, Y., Strohmer, T., and Voroninski, V. Phase retrieval via matrix completion. *SIAM J. Imaging Sci. 6*, 1 (2011), 199–225.
13. Deuflhard, P. *Newton Methods for Nonlinear Problems – Affine Invariance and Adaptative Algorithms*, 2nd ed., vol. 35 of *Springer Series in Computational Mathematics*. Springer, 2006.
14. Esser, J. E. *Primal-dual algorithm for convex models and applications to image restoration, registration and nonlocal inpainting*. PhD Thesis, University of California, Los Angeles, Los Angeles, USA, 2010.
15. Fazel, M. Matrix rank minimization with applications. *Elec Eng Dept Stanford University 54* (2002), 1–130.
16. Goldfarb, D., and Ma, S. Convergence of fixed-point continuation algorithms for matrix rank minimization. *Foundations of Computational Mathematics 11*, 2 (2011), 183–210.
17. Golub, G., and Loan, C. *Matrix Computations*, 3rd ed. Johns Hopkins University Press, Baltimore, 1996.
18. Golub, G. H., and Pereyra, V. The differentiation of pseudo-inverses and nonlinear least squares problems whose variables separate. *SIAM J. Numer. Anal. 10*, 2 (1973), 413–432.
19. Gonzalez, E. F., and Zhang, Y. Accelerating the lee-seung algorithm for non-negative matrix factorization. *Dept. Comput. & Appl. Math., Rice Univ., Houston, TX, Tech. Rep. TR-05-02* (2005).
20. Grasedyck, L., Kressner, D., and Tobler, C. A literature survey of low-rank tensor approximation techniques. *GAMM-Mitteilungen 36*, 1 (2013), 53–78.
21. Gross, D., Liu, Y.-K., Flammia, S., Becker, S., and Eisert, J. Quantum state tomography via compressed sensing. *Physical review letters 105*, 15 (2010), 150401.
22. Huang, J., Zhang, T., and Metaxas, D. Learning with structured sparsity. *J. Mach. Learn. Res. 12* (2011), 3371–3412.
23. Jaggi, M. Revisiting Frank-Wolfe: Projection-Free Sparse Convex Optimization. *JMLR W&CP 28*, 1 (2013), 427–435.
24. Johnson, C. R. Matrix completion problems: a survey. In *Matrix theory and applications* (1990), vol. 40, Providence, RI, pp. 171–198.
25. Keshavan, R. H., and Oh, S. A gradient descent algorithm on the grassman manifold for matrix completion. *arXiv preprint arXiv:0910.5260* (2009).
26. Kyrillidis, A., Baldassarre, L., El Halabi, M., Tran-Dinh, Q., and Cevher, V. Structured sparsity: Discrete and convex approaches. In *Compressed Sensing and its Applications*. Springer, 2015, pp. 341–387.

27. Kyrillidis, A., and Cevher, V. Matrix recipes for hard thresholding methods. *Journal Math. Imaging Vis. 48*, 2 (2014), 235–265.
28. Li, G., and Pong, T.-K. Global convergence of splitting methods for nonconvex composite optimization. *SIAM J. Optim. 25*, 4 (2015), 2434–2460.
29. Lin, Z., Chen, M., Wu, L., and Ma, Y. The Augmented Lagrange Multiplier Method for Exact Recovery of Corrupted Low-Rank Matrices. *UIUC Technical Report UILU-ENG-09-2215* (2009).
30. Liu, X., Wen, Z., and Zhang, Y. An efficient Gauss-Newton algorithm for symmetric low-rank product matrix approximations. *SIAM J. Optim.*, 3 (2015), 1571–1608.
31. Natarajan, B. K. Sparse approximate solutions to linear systems. *SIAM J. Comput. 24*, 2 (1995), 227–234.
32. Nesterov, Y. *Introductory lectures on convex optimization: A basic course*, vol. 87 of *Applied Optimization*. Kluwer Academic Publishers, 2004.
33. Nocedal, J., and Wright, S. *Numerical Optimization*, 2 ed. Springer Series in Operations Research and Financial Engineering. Springer, 2006.
34. Recht, B., Fazel, M., and Parrilo, P. Guaranteed minimum-rank solutions of linear matrix equations via nuclear norm minimization. *SIAM Review 52*, 3 (2010), 471–501.
35. Shen, Y., Wen, Z., and Zhang, Y. Augmented Lagrangian alternating direction method for matrix separation based on low-rank factorization. *Optim. Method and Softw.* (2012).
36. Signoretto, M., Tran-Dinh, Q., De-Lathauwer, L., and Suykens, J. Learning with Tensors: a framework based on convex optimization and spectral regularization. *J. Machine Learning 94*, 3 (2014), 303–351.
37. Toh, K.-C., and Yun, S. An accelerated proximal gradient algorithm for nuclear norm regularized linear least squares problems. *Pacific J. Optim. 6*, 615-640 (2010), 15.
38. Vandereycken, B. Low-rank matrix completion by Riemannian optimization. *SIAM J. Optim. 23*, 2 (2013), 1214–1236.
39. Wang, Y., Yin, W., and Zeng, J. Global convergence of ADMM in nonconvex nonsmooth optimization. *arXiv preprint arXiv:1511.06324* (2015).
40. Wen, Z., Yin, W., and Zhang, Y. Solving a low-rank factorization model for matrix completion by a nonlinear successive over-relaxation algorithm. *Math. Program. Comput. 4*, 4 (2012), 333–361.
41. Yu, H.-F., Hsieh, C.-J., Si, S., and Dhillon, I. S. Parallel matrix factorization for recommender systems. *Knowledge and Information Systems 41*, 3 (2014), 793–819.
42. Yu, Y. *Fast gradient algorithms for structured sparsity.* Phd thesis, University of Alberta, 2014.